

**ENGINEERING OF DAMAGE  
IN  
ION IMPLANTED SILICON**

**PROEFSCHRIFT**

TER VERKRIJGING VAN DE GRAAD VAN DOCTOR  
AAN DE UNIVERSITEIT TWENTE, OP GEZAG VAN  
DE RECTOR MAGNIFICUS, PROF. DR. IR. J.H.A.  
DE SMIT, VOLGENS BESLUIT VAN HET COLLEGE  
VAN DEKANEN IN HET OPENBAAR TE  
VERDEDIGEN OP DONDERDAG 18 JUNI 1992 TE  
16.00 UUR

DOOR

**JAN REINDER LIEFTING**

GEBOREN OP 9 APRIL 1962 TE GRONINGEN

Dit proefschrift is goedgekeurd door de promotoren

prof. dr. H. Wallinga,

prof. dr. F.W. Saris

en assistent-promotor

dr. J.S. Custer.

aan zuster Sonja

The work described in this thesis is part of the research program of the Stichting voor Fundamenteel Onderzoek der Materie (FOM) and was performed at the FOM-Instituut voor Atoom- en Molecuulfysica, Kruislaan 407, 1098 SJ Amsterdam, and the Faculty of Electrical Engineering, University of Twente, P.O. Box 217, 7500 AE, Enschede, The Netherlands. The work was made possible by financial support from the Nederlandse organisatie voor Wetenschappelijk Onderzoek (NWO) and Varian Ion Implant Systems (Gloucester, MA, USA).

CIP-DATA KONINKLIJKE BIBLIOTHEEK, DEN HAAG

Liefting, Jan Reinder

Engineering of damage in ion implanted silicon /

Jan Reinder Liefting. - [S.l. : s.n.]. - Ill.

Thesis Enschede. - With ref.

- Met samenvatting in het Nederlands.

ISBN 90-9005097-3

Subject: semiconductor technology / ion implantation / Si / damage engineering

© 1992 by Reinoud Liefting



# CONTENTS

1 INTRODUCTION: ION IMPLANTATION INTO Si	11
1 Introduction	11
2 Ion implant damage	11
3 Illustration of the criterion for dislocation formation	12
4 This thesis	15
2 DISLOCATION FORMATION IN Si IMPLANTED AT DIFFERENT TEMPERATURES	19
1 Introduction	20
2 Experimental	22
3 Pre-amorphization damage for low (B) and high (In) mass implants	22
3.1 B implants	22
3.2 In implants	26
3.3 Combined B and In implants	32
4 Pre-amorphization damage vs EOR-loop formation	35
5 EOR-loop formation for Ge implanted at RT and LN <sub>2</sub>	37
6 Conclusions	39
3 AVOIDING DISLOCATION FORMATION FOR B, P, AND As IMPLANTS IN SILICON	43
1 Introduction	44
2 Experimental	44
3 Results and discussion	44
4 Conclusions	51

4	CARBON IMPLANTATION FOR SUPPRESSION OF DISLOCATION FORMATION	53
1	Introduction	54
2	Experimental	54
3	Results	55
4	Discussion and conclusions	61
5	IMPROVED DEVICE PERFORMANCE BY MULTI STEP OR CARBON CO-IMPLANTS	65
1	Introduction	66
2	Sample preparation	69
3	Electrical measurements	71
4	Discussion and conclusions	76
6	GETTERING OF Cu AT BURIED DAMAGE LAYERS MADE BY Si SELF IMPLANTATION	81
1	Introduction	82
2	Experimental	82
3	Results and discussion	83
4	Conclusions	91
	SUMMARY	93
	SAMENVATTING	95
	NAWOORD	97
	CURRICULUM VITAE	99
	PUBLICATIONS	100



# CHAPTER 1

---

## INTRODUCTION: ION IMPLANTATION INTO Si

### 1. INTRODUCTION

Ion implantation technology is used in the semiconductor industry for introducing dopants into silicon [1]. The main advantage of ion implantation is the reproducibility of the dose and position of the introduced dopants. The major drawback are the secondary defects (e.g. dislocations) which form during the thermal treatment required to eliminate the crystal damage and activate the dopants [2-6]. These secondary defects can be detrimental to device performance, particularly if impurities are associated with the dislocation [7-9]. If dislocations occur in the depletion region of a *pn* junction, they can introduce a large density of generation-recombination centers, giving rise to large leakage current densities. In bipolar transistors, dislocations can also act as a 'diffusion pipe' along which the emitter or collector dopant can diffuse, resulting in a short between the emitter and collector [10]. Therefore, much effort has been put into determining how secondary defects form [4,6,11-13], what implant and anneal procedures can be used to minimize or avoid the formation of the secondary defects [14-18], and how dislocations can be made electrically harmless [7].

### 2. ION IMPLANT DAMAGE

Implanted ions come to rest by electronic and nuclear stopping mechanisms. The electronic stopping mechanism involves only excitation of electrons, whereas the nuclear stopping mechanism is caused by energetic collisions with the silicon host atoms. These host atoms are displaced if a threshold energy,  $\sim 15$  eV, is

transferred [19]. If much more than 15 eV is transferred, the host atom will consequently displace other Si atoms and a damage cascade results. The total number of displaced Si atoms depends strongly on the mass of the implanted ion and the implant energy [6]. Typical numbers of displaced Si atoms per implanted ion are, according to the Monte Carlo simulation program TRIM86, 250 for 50 keV  $^{11}\text{B}$  and 8800 for 1 MeV  $^{115}\text{In}$  [20].

For low mass implants, the displacement cascade densities are low and generally only simple vacancy/interstitial pairs are formed. These point defects are not stable at room temperature (RT); e.g. Si interstitials are mobile at temperatures above 4 K [21]. Hence, these point defects will either recombine or form larger point defect clusters. Such clusters will also form for high mass implants, but in addition amorphous zones may be created due to the high cascade densities [20]. The configuration of defect complexes and amorphous zones remaining after the implant is called the primary damage.

During a high temperature anneal (typically between 800 and 1200°C), more than 99% of this primary damage disappears [4]. The amorphous zones recrystallize and the point defect clusters dissolve. However, some of the interstitial clusters grow by capturing interstitials from other dissolving clusters. These interstitial clusters may grow large enough to form stable extrinsic dislocation loops, the secondary defects. It has been shown that dislocations form only if the implant generates a critical amount of primary damage as measured by Rutherford backscattering spectrometry (RBS) [6]. This criterion for dislocation formation has been demonstrated for RT implants of ions ranging from low mass (B) to high mass (In,Sb). The critical amount of primary damage is  $\sim 10^{16}$  /cm<sup>2</sup> displaced Si atoms for B but  $\sim 10^{17}$  /cm<sup>2</sup> for In or Sb implants. This 10x difference was attributed to the difference in primary damage morphology for the B and Sb implants.

### 3. ILLUSTRATION OF THE CRITERION FOR DISLOCATION FORMATION

Silicon was implanted with 1 MeV  $^{115}\text{In}$  to doses of 1.5 and  $2.0 \times 10^{13}$  /cm<sup>2</sup>. The displacement profiles generated by these implants, measured by RBS, show only a small difference, see Fig. 1. These samples were annealed at 900°C to remove the primary damage. Anneals for 5, 20, 60, and 300 sec were performed in a rapid thermal annealer (RTA), while the 15 min anneal was performed in a vacuum furnace.

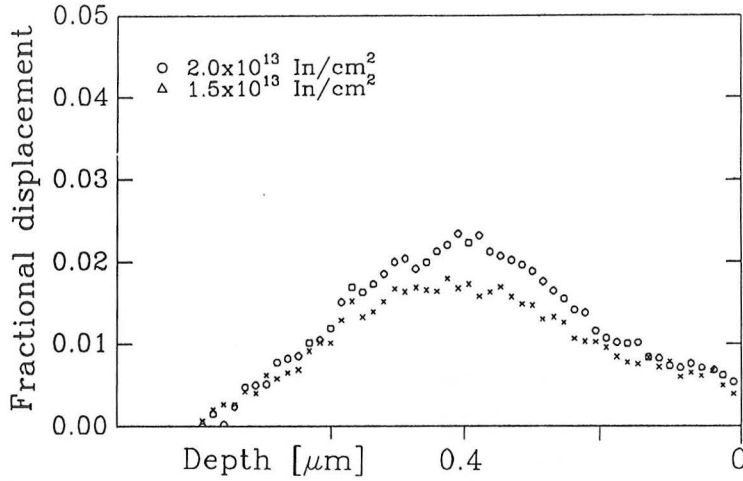


Fig. 1. Displacement damage profiles in Si after 1 MeV In implants to doses of 1.5 or  $2.0 \times 10^{13} / \text{cm}^2$ .

Figure 2 shows a cross-section transmission electron microscopy (XTEM) study of the recovery of the damage as a function of the anneal time. After the 5 sec anneal, both doses result in the formation of a very high concentration,  $\sim 10^{11} / \text{cm}^2$ , of dislocation rods. These rods are only 10 nm, and represent an early stage in the dislocation formation process [12]. Larger rods and some small dislocation loops are also visible in the micrographs. After 20 sec, a large difference is observed, with the low dose sample containing only a few loops, whereas this number is much higher for  $2.0 \times 10^{13} \text{ In/cm}^2$ . If the anneal is done for 60 sec, for the low In dose only one dislocation is observed, whereas the sample with the high dose is essentially unchanged compared to the 20 sec anneal. Clearly, a stable defect configuration is obtained for an In dose of  $2.0 \times 10^{13} / \text{cm}^2$ , whereas the dislocations formed for  $1.5 \times 10^{13} \text{ In/cm}^2$  are too small to be stable at  $900^\circ\text{C}$ . This is confirmed if the anneal time is prolonged to 5 or 15 min. No dislocations are observed in the low dose sample, while they remain for the high dose.

The principal of the criterion for dislocation formation is clearly demonstrated in this example. Primary damage amounts differing by only 30% were generated by In implants. For short anneal times, roughly the same type of dislocation rods are observed for both implants. The number of rods is higher for  $2.0 \times 10^{13} \text{ In/cm}^2$ . However, these rods are an early stage in the dislocation formation process and are not stable. Some of the rods will grow on the expense of others, and will turn into loops. Loops smaller than a critical size are not stable at  $900^\circ\text{C}$  and will

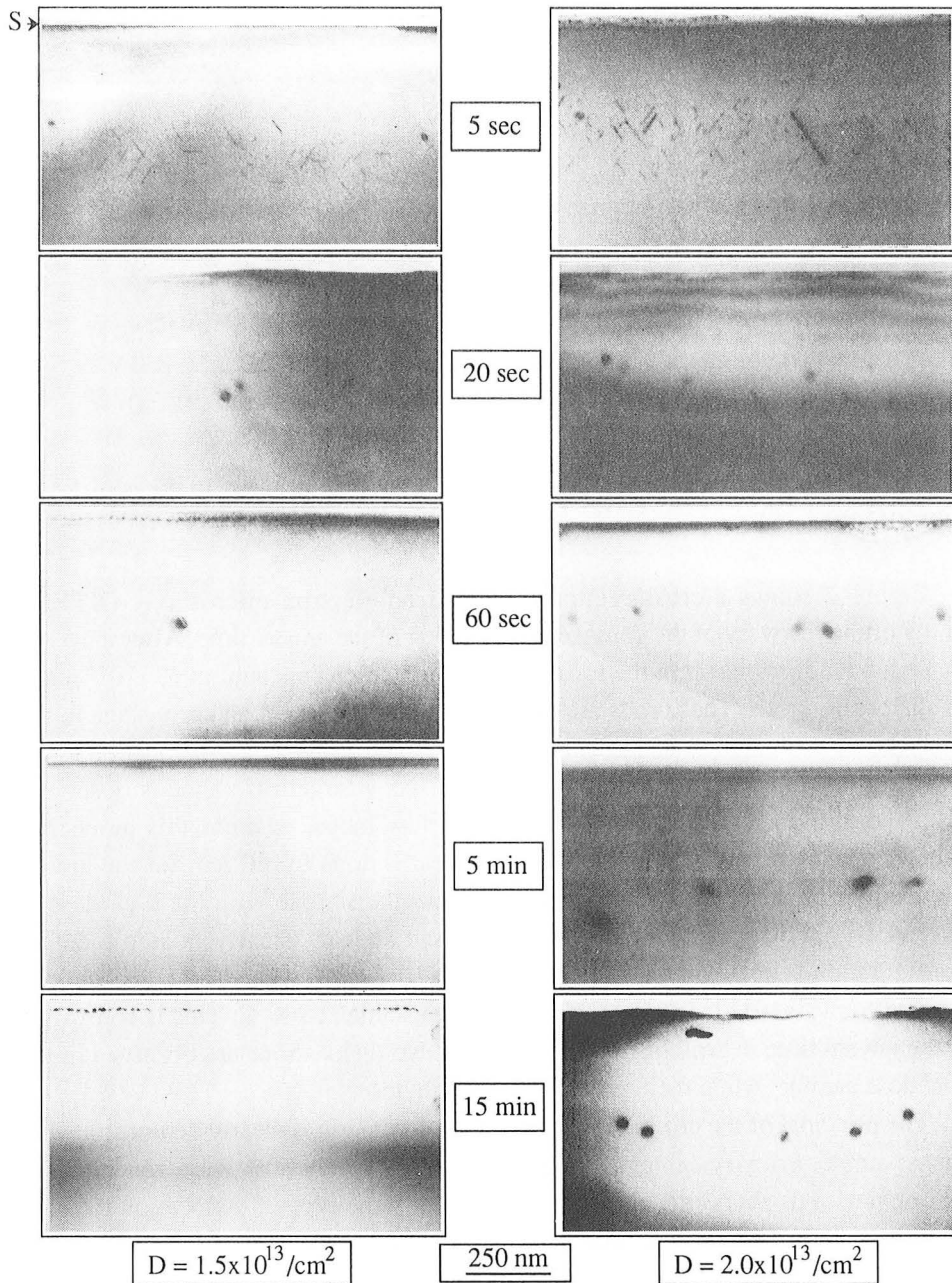


Fig. 2. XTEM micrographs after 900°C annealing of Si implanted with 1 MeV In to doses of  $1.5 \times 10^{13} / \text{cm}^2$  or  $2.0 \times 10^{13} / \text{cm}^2$ . Anneal times are indicated in the figure.

disappear if the anneal is continued [23]. This is the case for the  $1.5 \times 10^{13}$  /cm<sup>2</sup> In implant, whereas somewhat larger loops have formed for the  $2.0 \times 10^{13}$  /cm<sup>2</sup> In implant. Therefore, for the highest In dose, dislocations are still observed if the anneal is carried out for 15 min.

#### **4. THIS THESIS**

Recently, it was discovered that dislocations form only if during implantation a critical amount of primary damage is generated [6]. Since the criterion for dislocation formation is known, we also know how dislocations can be avoided. This thesis investigates several ways of engineering primary implant damage such that dislocations are formed or avoided when necessary.

In chapter 2, results of engineering the primary damage for low and high mass implants by performing the implants at elevated temperatures is presented. Implanting in this way enhances annealing during the implant and consequently reduces the amount of primary damage. It is investigated if engineering the primary damage in this way influences dislocation formation.

In chapter 3, TEM analysis of implants to doses which generate a total damage much higher than the critical amount are discussed. The implants are done either in 1 step, or in multiple steps, where each step is followed by an anneal. These implants generate roughly the same total amount of damage, but still dislocation formation should be different and this is studied.

We know that small interstitial clusters, formed during the implant, become stable dislocation loops by absorbing Si interstitials. Thus, dislocation formation could be engineered if we can introduce alternative sinks for the interstitials. It is thought that carbon can act as such a sink. For damage engineering, it is important to know how effective C is as a sink. This is investigated in chapter 4.

Dislocations can severely degrade the yield and quality of microelectronic devices. Several ways to avoid dislocation formation were discussed in the previous chapters. In chapter 5, these ways of damage engineering are introduced in a bipolar transistor fabrication process to investigate if device performance may be improved.

Until now, defects are considered to have only a negative influence on the quality of Si. This is correct if the defects trap metallic impurities and are positioned in the active regions of a device. By engineering the position of dislocations, the metallic impurities can be placed in regions where they do not influence device performance. Chapter 6 shows how this may be achieved.

## REFERENCES

- [1] S. Namba, ed., *Ion Implantation in Semiconductors* (Plenum Press, New York, 1975).
- [2] R.S. Nelson, in: *Proceedings European Conference on Ion Implantation*, Reading, England, p. 212 (1970).
- [3] S. Mader, in: *Ion Implantation Techniques*, eds. by H. Ryssel and H. Glawischnig, (Springer, Berlin, 1982).
- [4] K.S. Jones, S. Prussin, and E.R. Weber, *Appl. Phys. A* **45**, 1 (1988).
- [5] M. Tamura, *Mater. Sci. Rept.* **6**, 141 (1991).
- [6] R.J. Schreutelkamp, J.S. Custer, J.R. Liefiting, W.X. Lu, and F.W. Saris, *Mater. Sci. Rept.* **6**, 275 (1991).
- [7] K.V. Ravi, in: *Imperfections and Impurities in Semiconductor Silicon* (John Wiley & Sons, New York, 1981).
- [8] B.O. Kolbesen, W. Bergholz, H. Cerva, B. Fiegl, F. Gelsdorf, and G. Zoth, *Nucl. Instr. and Meth.* **B55**, 124 (1991).
- [9] K.H. Küsters, H.M. Mühlhoff, and H. Cerva, *Nucl. Instr. and Meth.* **B55**, 9 (1991).
- [10] F.W. Ragay, Ph. D. dissertation, (University of Twente, The Netherlands, 1991).
- [11] F.F. Morehead and B.L. Crowder, *Radiat. Eff.* **6**, 27 (1970).
- [12] T.Y. Tan, *Mater. Res. Soc. Symp. Proc.* **2**, 163 (1981).
- [13] K. Seshan and J. Washburn, *Radiat. Eff.* **37**, 147 (1978).
- [14] M. Servidori and I. Vecchi, *Solid-State Electron.* **24**, 329 (1981).
- [15] W.X. Lu, Y.H. Qian, R.H. Tian, Z.L. Wang, R.J. Schreutelkamp, J.R. Liefiting, and F.W. Saris, *Appl. Phys. Lett.* **55**, 1838 (1989).
- [16] R.J. Schreutelkamp, J.S. Custer, J.R. Liefiting, and F.W. Saris, *Appl. Phys. Lett.* **58**, 2827 (1991).
- [17] J.R. Liefiting, V. Raineri, J.S. Custer, R.J. Schreutelkamp, and F.W. Saris, *Mat. Res. Soc. Symp. Proc.* **235**, in press.
- [18] J.R. Liefiting, J.S. Custer, R.J. Schreutelkamp, and F.W. Saris, *Mat. Res. Soc. Symp. Proc.* **235**, in press.
- [19] G.H. Kinchin and R.S. Pease, *Rep. Prog. Phys.* **18**, 1 (1955).
- [20] J.P. Biersack and L.G. Haggmark, *Nucl. Instr. and Meth.* **174**, 257 (1980).
- [21] R.S. Nelson and D.J. Mazey, *International Conf. on Applications of Ion Beams to Semiconductor Technology*, Grenoble (1970).
- [22] M.O. Ruault, J. Chaumont, and H. Bernas, *Nucl. Instr. and Meth.* **209/210**, 351 (1983).

[23] I.R. Sanders and P.S. Dobson, *J. Mat. Sci.* **9**, 1987 (1974).



## CHAPTER 2

---

### DISLOCATION FORMATION IN Si IMPLANTED AT DIFFERENT TEMPERATURES

*The formation of pre-amorphization damage, i.e. dislocations formed by the agglomeration of Si interstitials, requires a minimum amount of implant damage. The amount of damage can be altered by changing implant temperature or current density, which can influence dislocation formation. We have studied this with cross-section transmission electron microscopy for B and In implants at keV and MeV energies. Dislocation formation for B implants, where only simple cascade densities are generated, does not depend on implant temperature or current density. For 1 MeV In implants, where the implant damage consists mainly of amorphous zones (a-zones), an increase in critical dose for dislocation formation by a factor of ~3 is observed if the implant temperature is raised. This is attributed to the interaction of point defects with the a-zones during the elevated temperature implant. Implants of 150 keV In at room temperature (RT) result in complete amorphization before the critical amount of crystal damage is reached. Here, end-of-range-loops (EOR-loops) form after annealing. Increasing the implant temperature suppresses amorphization, and pre-amorphization damage is observed if a critical amount of crystal damage has been generated. EOR-loop formation results from the agglomeration of Si interstitials from the amorphous/crystalline transition region. If the number of interstitials in this region is lowered by performing the implant at low temperature, EOR-loop formation can be suppressed. This is shown by comparing amorphizing Ge implants done at RT and liquid nitrogen temperature.*

## 1. INTRODUCTION

Ion implantation is commonly used for introducing dopants into silicon. The ions enter the substrate and come to rest in typically  $10^{-13}$  sec by nuclear and electronic stopping mechanisms [1]. The nuclear interactions give rise to displacements of Si host atoms. For low mass implants, the displacement cascade densities are low and generally only simple vacancy- and interstitial-related defects are created. These point defects are not stable at RT, thus they either recombine or form larger point defect clusters [2,3]. Such clusters form also for high mass implants, but in addition amorphous zones (a-zones) are created by the dense cascades [4]. The configuration of defect complexes and a-zones remaining after the implant is called the primary damage.

Annealing of primary damage below the amorphization threshold results in the formation of category I dislocations, also known as pre-amorphization damage, if a critical amount of primary damage has been exceeded [5]. This criterion for dislocation formation has been demonstrated for RT implants of ions ranging from low mass ( $^{11}\text{B}$ ) to high mass ( $^{115}\text{In}$ ,  $^{121}\text{Sb}$ ). The critical amount of primary damage corresponds to a number of displaced Si atoms of  $\sim 10^{16}$  / $\text{cm}^2$  for B and  $\sim 10^{17}$  / $\text{cm}^2$  for In implants, according to Rutherford backscattering spectrometry (RBS) and channeling analysis [5]. This difference in number was attributed to the difference in primary damage morphology for the B (simple point defect complexes) and In implants (also amorphous zones). The displaced Si atoms inside the a-zones do not contribute to dislocation formation because the a-zones recrystallize upon annealing.

Changing the amount of primary damage could result in a change in dislocation formation. The amount and type of primary damage is influenced by several parameters. (1) An increasing mass of the implanted ion results in a change from only point defect clusters for low mass ions to a damage morphology mainly consisting of a-zones for high mass ions [5,6]. (2) Implanting at higher energy distributes the primary damage over larger depth. For high mass implants, the critical amount of primary damage is then obtained before the amorphization threshold is reached [5]. (3) Performing the implant at an elevated temperature enhances annealing during the implant. For 1 MeV Si implants, an increase in implant temperature of  $30^\circ\text{C}$  can already reduce the amount of primary damage by 90% [7]. High mass implants, which normally result in amorphous surface layers for RT implants, generate only crystalline damage if the implant is performed at higher temperatures [8]. (4) The influence of the implant dose on the amount of primary damage is strongly dependent on the type of primary damage formed. A

linear dependence on implant dose is observed for high mass implants done at RT [8]. Implants of low mass ions or elevated temperature implants result in a damage build-up that is strongly non-linear with dose [6-8]. (5) Different ion fluxes give rise to different defect production rates in the silicon [7]. For a high defect production rate, it is easy for the point defects to interact and form larger complexes. For a low defect production rate, the point defects anneal before they can interact and form more stable defect complexes. Therefore, the highest amount of primary damage results from implants carried out with the highest flux. From the above, it is concluded that there are several ways to lower the amount of primary damage. Increasing the implant temperature or decreasing the ion flux may therefore help reduce dislocation formation.

For keV high mass implants carried out at room temperature (RT), the amorphization threshold is attained before the critical amount of primary damage is reached. However, amorphization is avoided if the implant is performed at a sufficiently high substrate temperature [8,9]. The primary damage then consists only of crystal damage. Again, a critical amount of crystal damage should be required to form dislocations during thermal treatment.

Annealing an amorphous layer results in the formation of end of range loops (EOR-loops) near the original amorphous/crystalline (a/c) transition region [6,10]. The extrinsic loops result from the agglomeration of Si interstitials which are positioned in the a/c transition region [11]. For a certain implant dose, the amount of crystal damage in this region can be lowered if the implant is done at lower temperature [12,13]. If the amount of damage is lower than a critical number, EOR-loop formation might be avoided [11]. Servidori *et al.* indeed showed that, for  $2 \times 10^{15} / \text{cm}^2$  100 keV P implants, dislocations were observed for RT implants, in contrast to implants performed at liquid nitrogen temperature (LN<sub>2</sub>) [14].

In the first part of this chapter, we report on dislocation formation for low (B) and high (In) mass implanted silicon. The primary damage for B implants was altered by changing the implant temperature and the implant flux. Only smaller point defect clusters are formed for these B implants, hence, only some annihilation and coarsening of the point defect clusters is expected. XTEM analysis will show the influence of this change in primary damage on dislocation formation. For comparison, the primary damage for In implants was also changed by performing the implants at different temperatures. Here, a larger influence on dislocation formation is expected, since a-zones are not stable at higher temperatures and could influence the point defect configuration. By comparing the results for the B and In implants, the influence of a-zones on dislocation formation can be determined.

The second part of this chapter discusses dislocation formation for low energy In implants. EOR-loops result from annealing the RT implants. Amorphization is avoided when the implant is performed at 300°C and pre-amorphization damage should be observed when the amount of crystal damage exceeds the critical amount.

Finally, in the third part of this chapter, it is shown that EOR-loop formation can be avoided. This is demonstrated for 75 keV Ge implants.

## 2. EXPERIMENTAL

Implants of  $^{11}\text{B}$ ,  $^{73}\text{Ge}$ , and  $^{115}\text{In}$  with energies between 75 keV and 1 MeV were done in 5-15  $\Omega\text{cm}$ ,  $p$ -type float zone (100) silicon in a random direction. A current density lower than 20 nA/cm<sup>2</sup> was used, unless otherwise specified. The samples (~15x15mm<sup>2</sup>) were mounted on a molybdenum or copper block cooled by liquid nitrogen or heated to temperatures up to 500°C by a tungsten filament. The temperature was monitored with a Pt100 resistor mounted in the molybdenum block or with a thermocouple mounted on the copper block. The number of displaced Si atoms in the as-implanted samples was determined using 2 MeV He<sup>+</sup> Rutherford backscattering spectrometry (RBS) in the channeling geometry [15]. The implanted samples were annealed in a vacuum furnace (base pressure  $\approx 10^{-7}$  Torr). Cross-section and plan-view transmission electron microscopy were done in the bright-field mode using a Siemens Elmiskop 101.

## 3. PRE-AMORPHIZATION DAMAGE FOR LOW (B) AND HIGH (In) MASS IMPLANTS

### 3.1 B implants

Dislocation formation was investigated for 200 keV and 1 MeV  $^{11}\text{B}$  implants. Figure 1 shows XTEM micrographs after 15 min, 900°C anneals of samples implanted with 200 keV B for different doses and implant temperatures. No dislocations are observed for a room temperature (RT) implant of  $0.7 \times 10^{14}$  B/cm<sup>2</sup>, but they are seen for  $1.0 \times 10^{14}$  B/cm<sup>2</sup>. Hence, the latter dose is the threshold dose which generates the critical amount of damage needed for dislocation formation for RT implants. If raising the implant temperature helped suppress dislocation formation, the threshold dose should increase for higher implant temperatures.

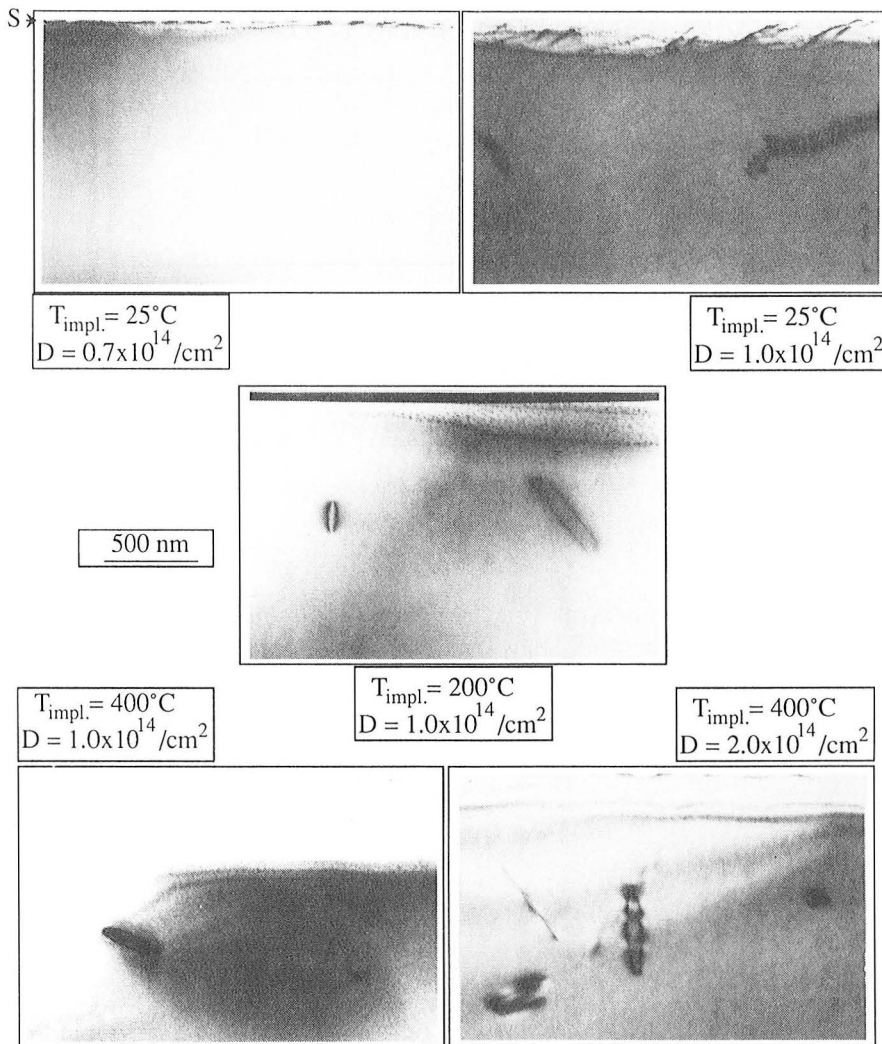


Fig. 1. XTEM micrographs of samples implanted with 200 keV  $^{11}\text{B}$  and annealed at  $900^\circ\text{C}$  for 15 min. Implant doses and temperatures are denoted in the figure.

However, dislocations are still observed for  $1.0 \times 10^{14} / \text{cm}^2$  B implants at either  $200$  or  $400^\circ\text{C}$ . The concentration of dislocations increases for the  $400^\circ\text{C}$  implant if the dose is raised to  $2.0 \times 10^{14} / \text{cm}^2$ . Thus, the dose required for dislocation formation for 200 keV B implants is not influenced if the implant temperature is raised from  $25$  to  $400^\circ\text{C}$ .

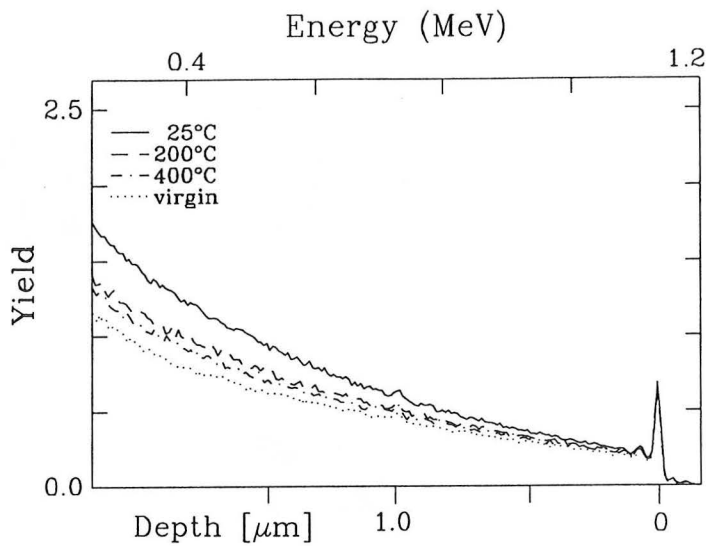


Fig. 2. RBS channeling spectra of Si implanted with  $5 \times 10^{14} / \text{cm}^2$  1 MeV B at 25, 200, or 400°C. A spectrum of unimplanted Si is shown for comparison.

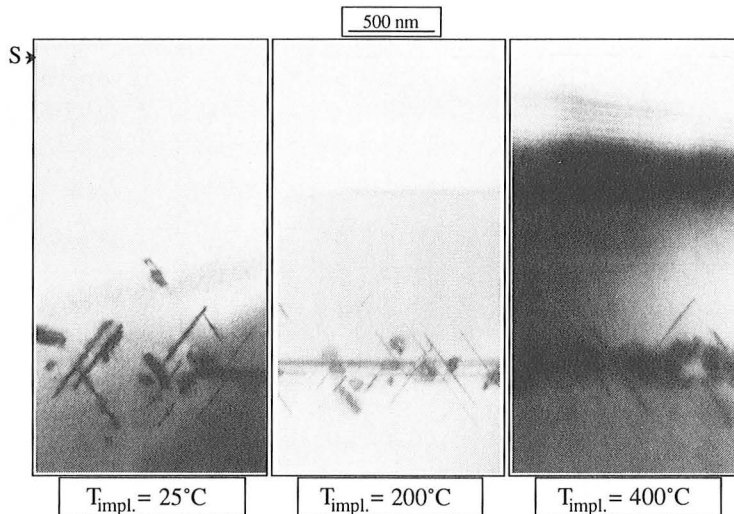


Fig. 3. XTEM of Si implanted with  $5 \times 10^{14} / \text{cm}^2$  1 MeV B at 25, 200, or 400°C. Annealing was done at 900°C for 15 min.

Implants of  $5 \times 10^{14} / \text{cm}^2$  1 MeV B were performed at temperatures ranging from 25 to 400°C. The beam current density on target was 15 nA/cm<sup>2</sup>. This dose generates ~8x the critical amount of damage required for dislocation formation for 1 MeV B implants [5]. RBS channeling spectra of the samples are shown in Fig. 2. Also shown is the spectrum of unimplanted Si. The dechanneling is highest for the RT implant and decreases for increasing temperature. Therefore, the RBS-measured primary damage is reduced if the implant is done at an elevated temperature.

XTEM micrographs of annealed samples implanted at 25, 200, and 400°C are presented in Fig. 3. The anneal was done at 900°C for 15 min. A band of elongated dislocation loops with lengths up to 1.0 μm and positioned at a depth of ~1.6 μm is observed for the RT implant. The micrographs for the 200 and 400°C implants do not show any reduction in dislocation formation. Again, raising the implant temperature does not influence dislocation formation for B implants, even though the primary damage levels measured by RBS were different.

Implants of  $5 \times 10^{14} / \text{cm}^2$  1 MeV B at 400°C were also performed at higher current densities of 150 and 1500 nA/cm<sup>2</sup>. RBS channeling measurements of these samples are presented in Fig. 4. The sample implanted at the lowest current density results in the lowest dechanneling yield. The highest yield, and thus the highest amount of primary damage, is found for the sample implanted at a current density

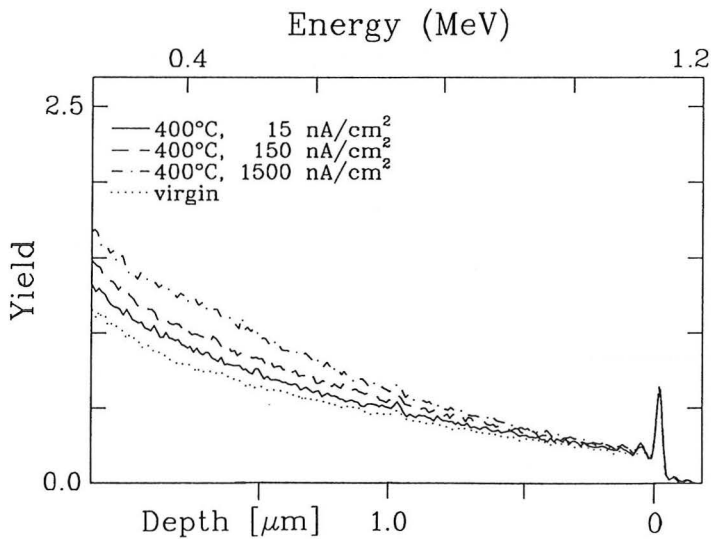


Fig. 4. RBS channeling spectra of Si implanted with  $5 \times 10^{14} / \text{cm}^2$  1 MeV B at 400°C for current densities of 15, 150, or 1500 nA/cm<sup>2</sup>. A channeling spectrum of unimplanted Si is shown for comparison.

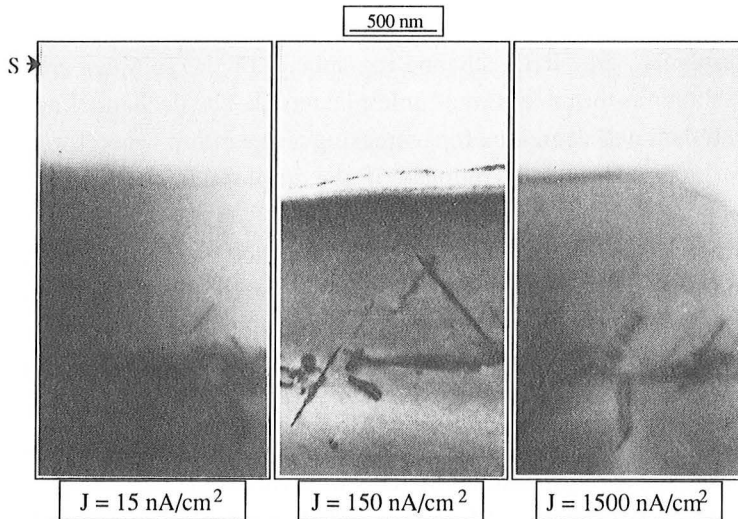


Fig. 5. XTEM of  $5 \times 10^{14} / \text{cm}^2$  1 MeV B implanted at  $400^\circ\text{C}$  for current densities of 15, 150, or  $1500 \text{ nA/cm}^2$ . Annealing was carried out at  $900^\circ\text{C}$  for 15 min.

of  $1500 \text{ nA/cm}^2$ . XTEM micrographs for these samples (Fig. 5) all show a band of elongated dislocations positioned at a depth of  $\sim 1.6 \mu\text{m}$  with no observable difference in dislocation size or density. Thus, changing the primary damage by changing the current density of the B implant does not seem to influence dislocation formation.

The only number which counts for dislocation formation for the B implants is the total number of Si atoms displaced during the implant. The structure of defect complexes formed during implantation, which was altered by changing either the implant temperature or the flux, is apparently not so critical.

### 3.2 In implants

Implants of high mass ions at RT result in high cascade densities which lead to the formation of amorphous zones (a-zones). By performing implants of In at elevated temperatures, the a-zones will decrease in size or may not form at all. This will also influence the diffusion and population of point defects, and a large change in primary damage is expected. By comparing results for B and In implants, the influence of a-zones on the point defect population and, therefore, on dislocation formation can be investigated.

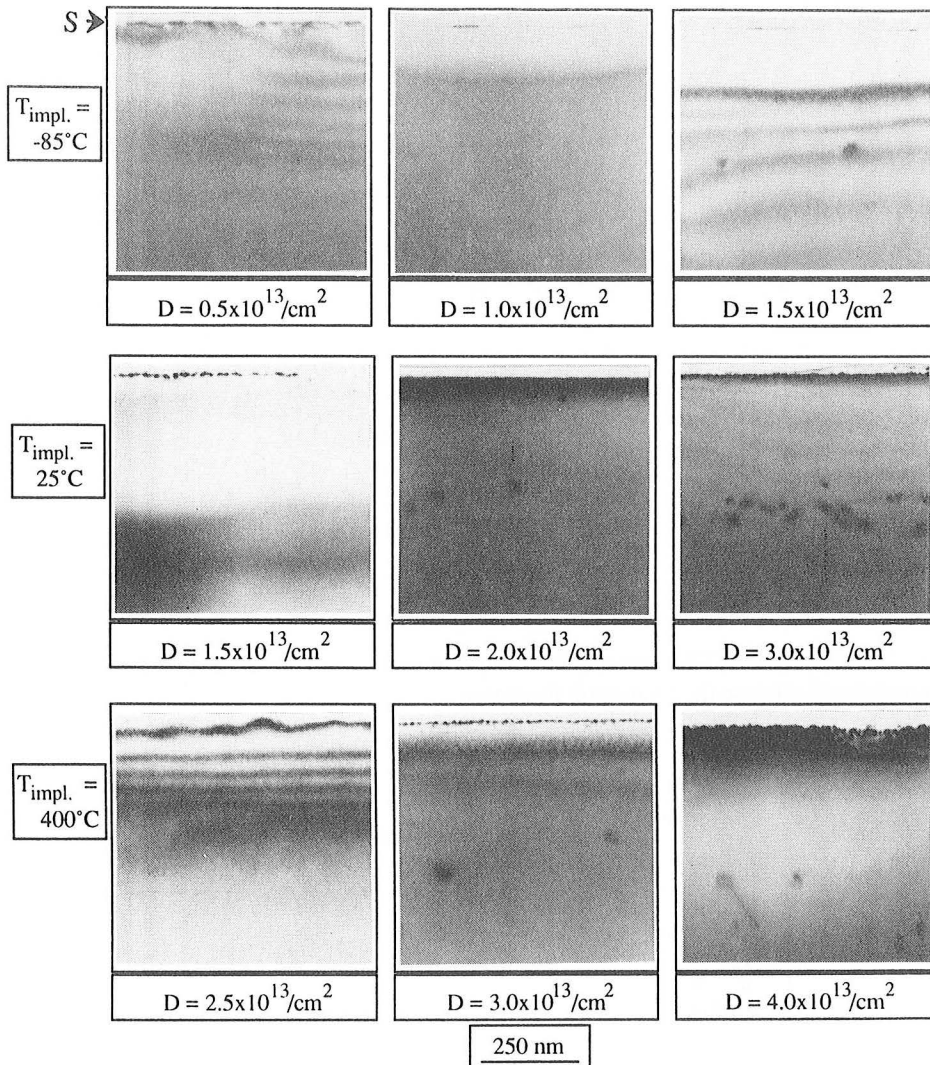


Fig. 6. XTEM of Si implanted with 1 MeV In at -85, 25, or 400°C for different doses. Annealing was done at 900°C for 15 min.

Figure 6 shows XTEM micrographs after annealing of samples implanted with 1 MeV  $^{115}\text{In}$  for different doses and implant temperatures. For implants at -85°C, no dislocations are observed for a dose of  $0.5 \times 10^{13} \text{ In/cm}^2$  after 900°C, 15 min annealing. Only one dislocation was found in the XTEM sample for a dose of  $1.0 \times 10^{13} \text{ In/cm}^2$ , while a band of dislocation loops at a depth of  $0.4 \mu\text{m}$  is observed for a dose of  $1.5 \times 10^{13} \text{ In/cm}^2$ . In contrast, dislocations for RT implants begin to appear only between  $1.5$  and  $2.0 \times 10^{13} \text{ In/cm}^2$ , in agreement with previous results [5]. The concentration of loops further increases for  $3.0 \times 10^{13} \text{ In/cm}^2$ . For

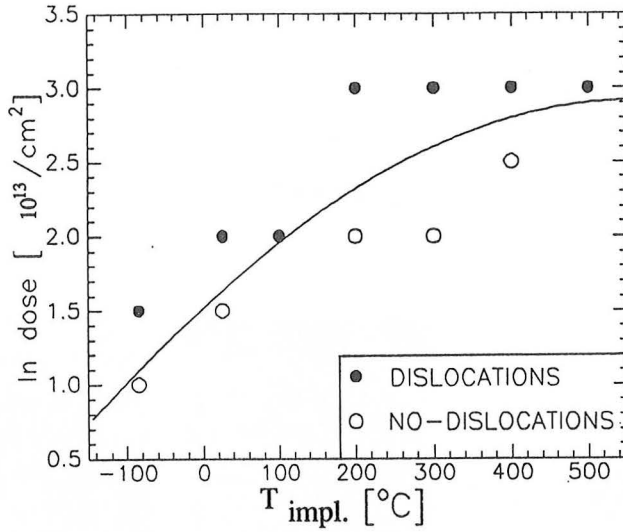


Fig. 7. Summary of XTEM results for 1 MeV In implants. The full drawn line gives the estimated critical dose for dislocation formation.

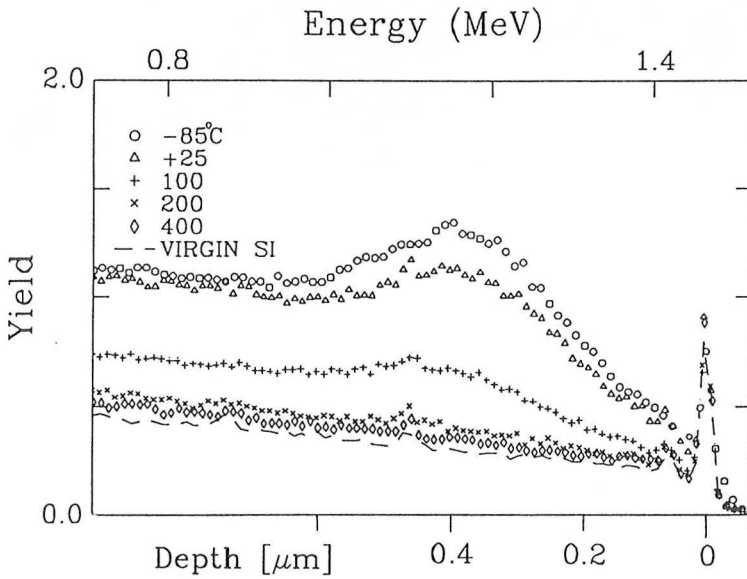


Fig. 8. RBS channeling spectra for In doses closest to the critical dose for dislocation formation.

TABLE I.

Overview of the implant doses and temperatures for the 1 MeV In implants, including the number of displaced Si atoms estimated from RBS and information concerning dislocation formation ( - no dislocations, + dislocations).

In dose [ $10^{13}/\text{cm}^2$ ]	implant temperature [°C]	Si <sub>displ.</sub> [/ $\text{cm}^2$ ]	dislocations
0.5	-85	$6.0 \times 10^{16}$	-
1.0	-85	$1.9 \times 10^{17}$	-/+
1.5	-85	$3.6 \times 10^{17}$	+
1.5	25	$1.5 \times 10^{17}$	-
2.0	25	$1.9 \times 10^{17}$	+
3.0	25	$3.6 \times 10^{17}$	+
2.0	100	$5.0 \times 10^{16}$	-/+
3.0	100	$8.1 \times 10^{16}$	+
4.0	100	$9.5 \times 10^{16}$	+
2.0	200	$2.4 \times 10^{16}$	-
3.0	200	$3.4 \times 10^{16}$	+
4.0	200	$3.5 \times 10^{16}$	+
2.0	300	$1.1 \times 10^{16}$	-
3.0	300	$1.1 \times 10^{16}$	+
4.0	300	$1.4 \times 10^{16}$	+
2.5	400	$0.9 \times 10^{16}$	-
3.0	400	$1.2 \times 10^{16}$	+
4.0	400	$1.4 \times 10^{16}$	+
3.0	500	$0.5 \times 10^{16}$	-
4.0	500	$0.4 \times 10^{16}$	+
6.0	500	$0.8 \times 10^{16}$	+
3.0	25	$3.6 \times 10^{17}$	+
3.0	25 & 400°C/3 hr	$4.7 \times 10^{16}$	+
3.0	400	$1.2 \times 10^{16}$	+

implants at 400°C, dislocations are not observed until a dose of  $3.0 \times 10^{13}$  In/cm<sup>2</sup>.

The results for temperatures ranging from -85°C to 500°C are summarized in Fig. 7. The In threshold dose for dislocation formation is represented by the drawn line and increases by a factor of ~3 across this temperature range, saturating at ~400°C.

Figure 8 shows RBS channeling spectra for In doses closest to the critical dose at several implant temperatures. The primary damage in the Si is highest for an implant at -85°C and consists of  $1.9 \times 10^{17}$  /cm<sup>2</sup> displaced Si atoms. This number is calculated by subtracting the dechanneling contribution from the total yield [15]. The number of displaced Si atoms estimated from the RBS spectra decreases with increasing implant temperature, see Table I. The critical number needed for dislocation formation was determined by combining the RBS and XTEM results. For RT implants, this number is  $1.9 \times 10^{17}$  /cm<sup>2</sup>, similar to previous results [5]. The critical number decreases by a factor of ~40 with increasing substrate temperature below  $10^{16}$  /cm<sup>2</sup> for implants done at 500°C. This number is close to the critical number found for B implants, in which case no a-zones are created [5].

At implant temperatures of ~400°C, isolated a-zones anneal out [9,16]. Such annealing of amorphous Si may influence the point defect population, and thereby dislocation formation. Annealing an In implanted sample at 400°C prior to the high

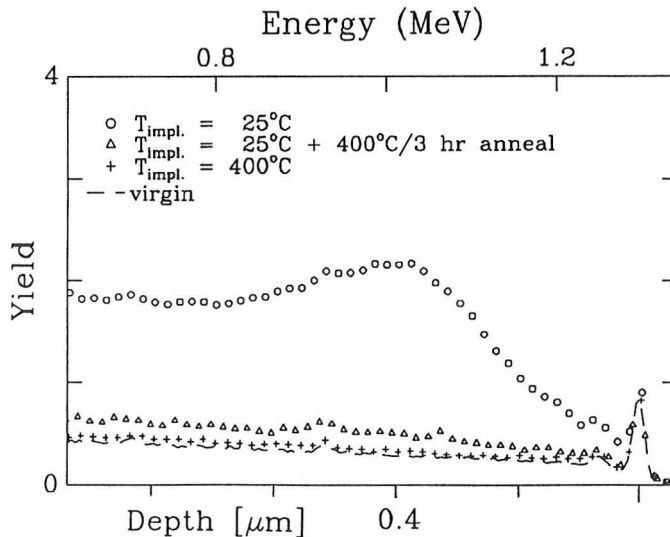


Fig. 9. RBS channeling spectra of Si implanted with  $3 \times 10^{13}$  /cm<sup>2</sup> 1 MeV In at RT or 400°C. Part of the RT implanted sample received an anneal at 400°C for 3 hr.

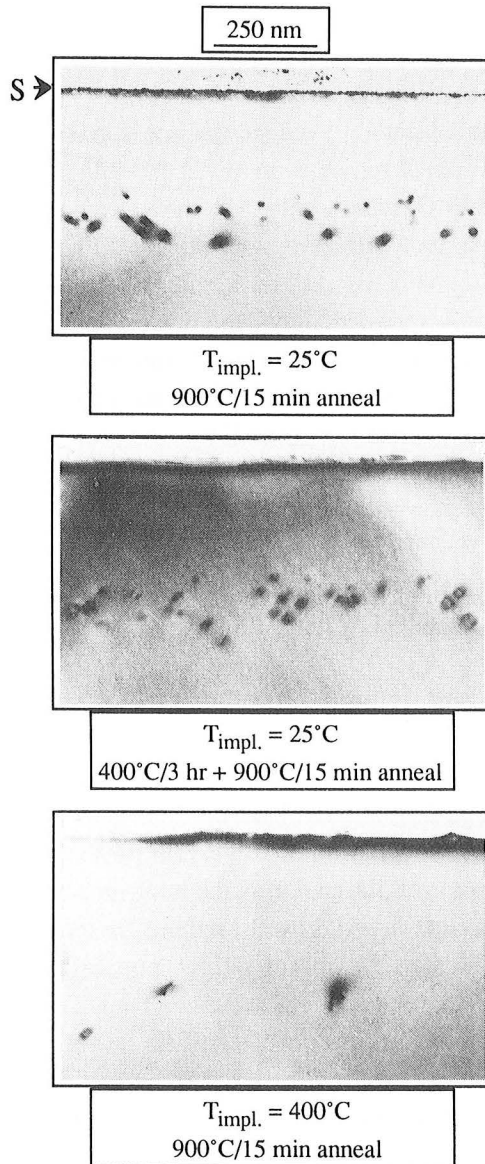


Fig. 10. XTEM micrographs of Si implanted with  $3 \times 10^{13} / \text{cm}^2$  1 MeV In after final annealing at 900°C for 15 min. Implant and anneal temperatures are denoted in the figure.

temperature treatment may also influence dislocation formation. Figure 9 shows RBS channeling spectra for  $3 \times 10^{13} / \text{cm}^2$  1 MeV In implants at 25 and 400°C. Part of the RT implanted sample was subsequently annealed at 400°C for 3 hr, much longer than the 0.5 hr needed for performing the implants. The highest dechanneling, found for the sample implanted at RT, peaks at a depth of 0.4  $\mu\text{m}$  and corresponds to  $\sim 3.6 \times 10^{17} / \text{cm}^2$  displaced Si atoms (Table I). Annealing this sample at 400°C for 3 hr substantially reduces the measured number of displaced Si atoms to  $4.7 \times 10^{16} / \text{cm}^2$ . However, an even lower dechanneling is observed for the sample *implanted* at 400°C, where only  $1.2 \times 10^{16} / \text{cm}^2$  displaced Si atoms are detected. This is in agreement with earlier results for 40 keV Sb implants, which also show a greater reduction in disorder for implants *done* at elevated temperature, as opposed to samples only annealed at higher temperatures [17].

XTEM micrographs of these samples after 15 min, 900°C anneals are shown in Fig. 10. A band with a high concentration of dislocation loops at a depth of 0.4  $\mu\text{m}$  is observed for both RT implanted samples. Thus, the pre-anneal at 400°C for 3 hr does not influence dislocation formation. However, XTEM analysis of the sample *implanted* at 400°C shows a much lower concentration of dislocation loops. Hence, only *performing* the 1 MeV In implant at elevated temperatures alters dislocation formation. This implies that annealing of the a-zones during the implant reduces the point defect population, and thereby helps suppress dislocation formation.

### 3.3 Combined B and In implants

For the 1 MeV In implants, a dependence of the critical dose for dislocation formation on implant temperature was observed. This is in contrast with the results for the B implants, where the only number relevant for dislocation formation was the total number of Si atoms displaced during the implant. The damage generated by In implants differs from that induced by B implants by the formation of a-zones, which apparently influences the point defect population and consequently dislocation formation. Sadana *et al.* suggested that a/c interfaces can act as traps for Si interstitials, leaving a lower number of interstitials for forming dislocations [18]. By analogy, amorphous zones could also act as interstitial traps. To test this, combined B and In implants were carried out to see whether (regrowing) a-zones trap interstitials. Indium was implanted at 1 MeV at RT to a dose of  $0.75 \times 10^{13} / \text{cm}^2$ , half the dose required for dislocation formation (Fig. 7). A significant fraction of the damage generated by this implant is in the form of a-zones. Next, 200 keV B was implanted to doses of either 0.7 or  $1.0 \times 10^{14} / \text{cm}^2$ . These B implants should only add simple point defects. (From Fig. 1, it can be

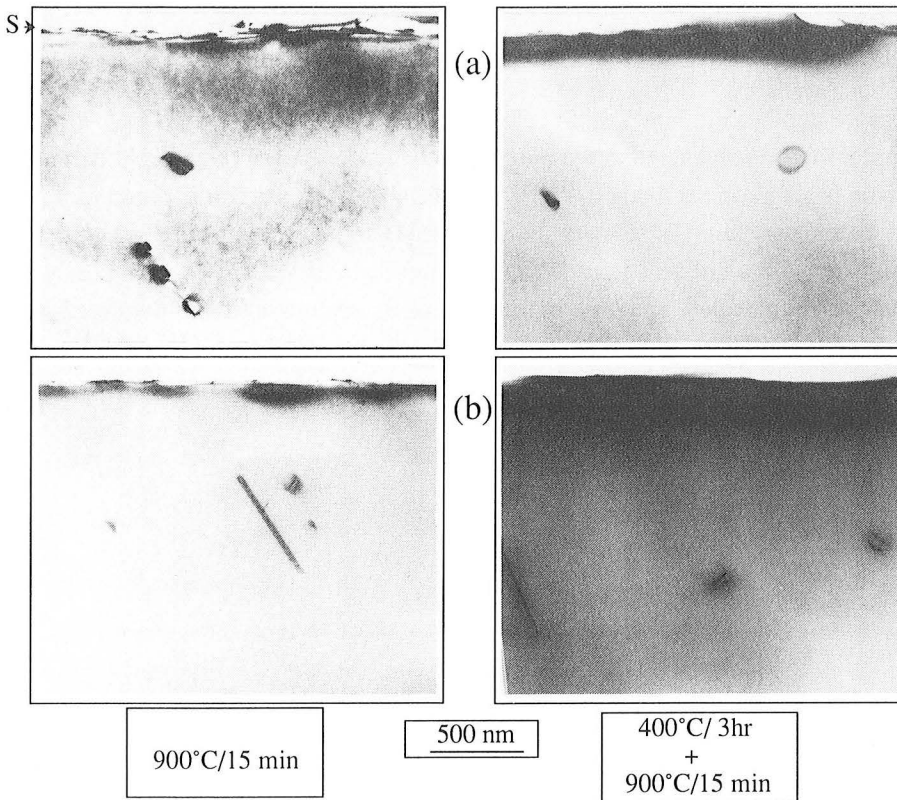


Fig. 11. XTEM micrographs after 900°C, 15 min annealing of samples implanted with  $0.75 \times 10^{13}$  /cm<sup>2</sup> 1 MeV In and 200 keV B to doses of (a)  $0.7 \times 10^{14}$  /cm<sup>2</sup> or (b)  $1.0 \times 10^{14}$  /cm<sup>2</sup>. Part of the samples first received an anneal at 400°C for 3 hr.

seen that  $0.7 \times 10^{14}$  is just below, and  $1.0 \times 10^{14}$  /cm<sup>2</sup> just above, the critical dose for dislocation formation for single implants.) If the a-zones generated by the In implant would trap a significant number of the interstitials created by the B implant, then dislocations should not form for either implant. Parts of these samples first received an anneal at 400°C for 3 hr. The largest a-zones will not regrow during this anneal [4], while the interstitials will be highly mobile. Hence, interstitials should be able to diffuse and interact with the a-zones.

XTEM micrographs of the samples after the final 900°C anneal for 15 min are presented in Fig. 11. Dislocations are observed not only for the sample which was implanted with  $1.0 \times 10^{14}$  B/cm<sup>2</sup>, but also for the sample with the sub-critical B dose of  $0.7 \times 10^{14}$  In/cm<sup>2</sup>. The number of defects found is highest for the B dose of  $1.0 \times 10^{14}$  /cm<sup>2</sup>. If a pre-anneal at 400°C is carried out, the same density of

dislocations is observed. Therefore, even if a-zones are in the vicinity of highly mobile interstitials, they have no influence on dislocation formation. From these results it is concluded that a-zones are not efficient traps for interstitials created by its own, or another implant.

Implanting In at elevated temperature affects the formation of amorphous Si and therefore has a strong influence on damage formation. In the complicated build-up and dynamic annealing of primary damage for high mass implants, the point defect population can also be altered, which consequently influences dislocation formation. For elevated temperature implants of B, the interaction of damage is less complicated and dislocation formation is not influenced by increasing the implant temperature.

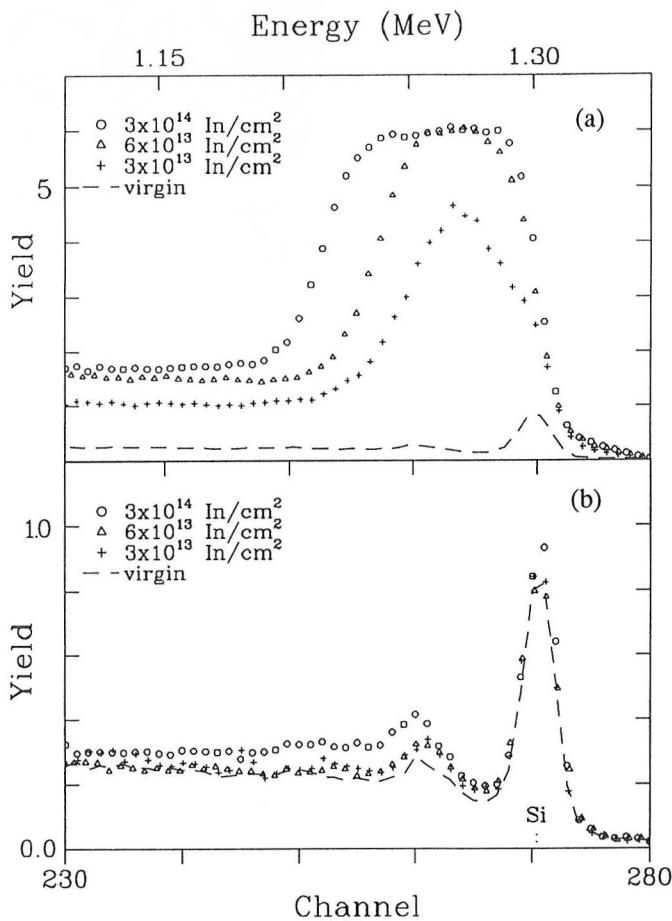


Fig. 12. RBS channeling spectra before annealing for 150 keV In implants done at RT or 300°C. Doses and implant temperatures are indicated in the figure.

#### 4. PRE-AMORPHIZATION DAMAGE vs EOR-LOOP FORMATION

For RT implants of 150 keV In, amorphization takes place before the critical number of Si atoms needed for dislocation formation is displaced, and end-of-range dislocation loops (EOR-loops) are observed after annealing [5,6]. However, if these implants are carried out at an elevated temperature, amorphization should be suppressed and pre-amorphization damage may result instead.

Figure 12 shows RBS channeling spectra of 150 keV In implants done at 25 and 300°C for doses of  $3 \times 10^{14}$ ,  $6 \times 10^{13}$ , and  $3 \times 10^{13}$  In/cm<sup>2</sup>. The implant of  $3 \times 10^{14}$  /cm<sup>2</sup> In at RT creates a 110 nm thick amorphous surface layer. If the In dose is lowered to  $6 \times 10^{13}$  /cm<sup>2</sup>, only a buried amorphous layer is formed. In the case of the lowest dose,  $3 \times 10^{13}$  /cm<sup>2</sup>, the dechanneling yield does not reach the random level, indicating that a highly damaged silicon region has formed. In contrast, for the 300°C implants, only small direct scattering peaks are observed by RBS. The number of displaced Si atoms for the 25 and 300°C implants are given in Table II. For both temperatures, the number increases with increasing dose.

Figure 13 shows XTEM micrographs of these samples after 900°C, 15 min annealing. The  $3 \times 10^{14}$  In/cm<sup>2</sup> RT implant leads to the formation of two defect bands. One band is located near the original amorphous/crystal interface and consists of EOR-loops with a density of  $\sim 2 \times 10^{10}$  /cm<sup>2</sup>, and the second consists of small In precipitates near the projected range ( $R_p = 40$  nm) of the In [19,20]. XTEM of the as-implanted sample for an In dose of  $6 \times 10^{13}$  /cm<sup>2</sup> shows the formation of a 30 nm thick buried amorphous layer. Heavily damaged crystalline Si

TABLE II.

Overview of the implant doses and temperatures for the 150 keV In implants, including the number of displaced Si atoms estimated from RBS and information concerning dislocation formation (- no dislocations, + dislocations).

In dose [10 <sup>13</sup> /cm <sup>2</sup> ]	T <sub>impl.</sub> [°C]	Si <sub>displ.</sub> [/cm <sup>2</sup> ]	dislocations
3	25	$2.8 \times 10^{17}$	+
6	25	$4.6 \times 10^{17}$	+
30	25	$6.2 \times 10^{17}$	+
3	300	$3.2 \times 10^{15}$	-
6	300	$3.5 \times 10^{15}$	+
30	300	$9.9 \times 10^{15}$	+

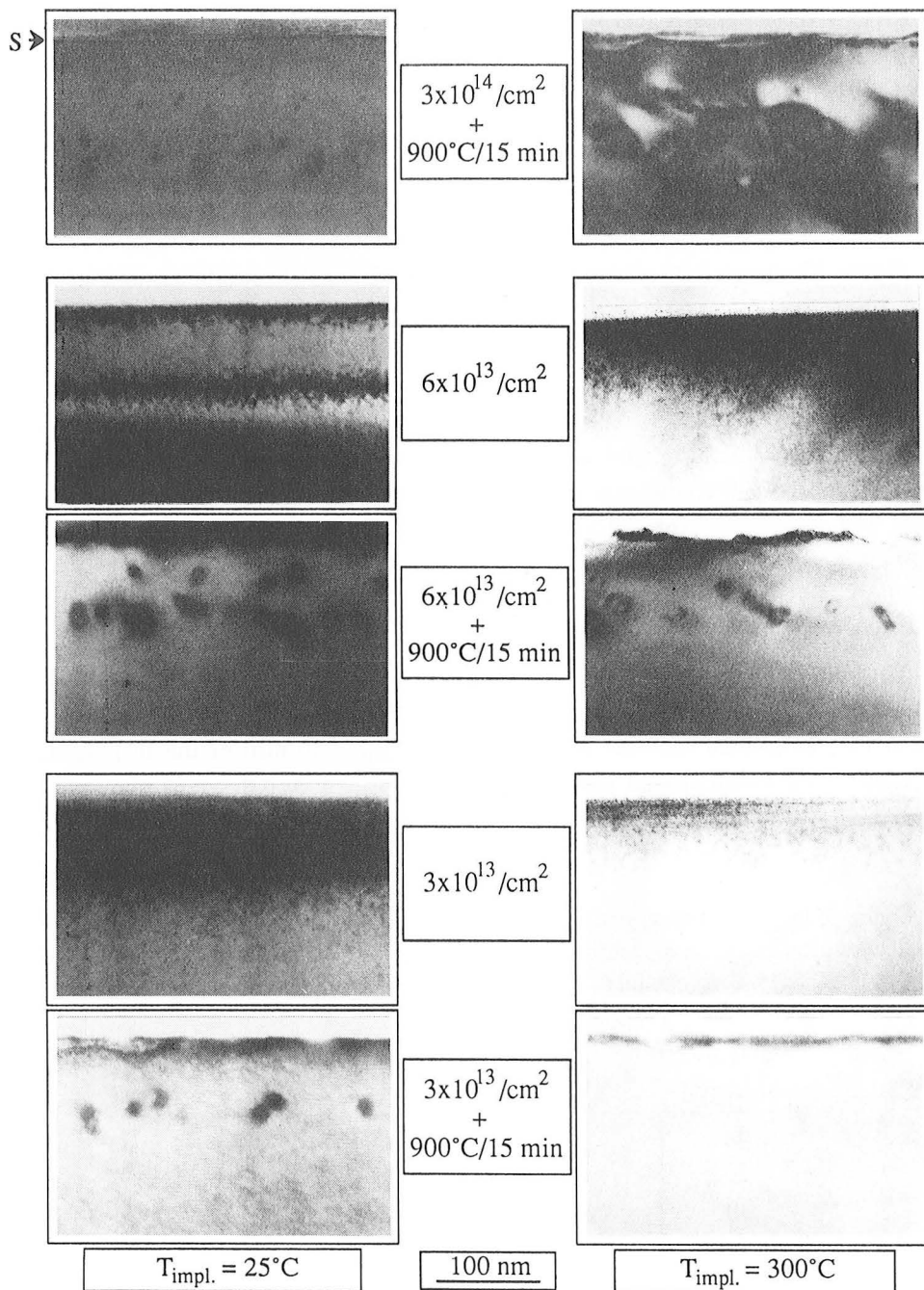


Fig. 13. XTEM of Si implanted with 150 keV In at 25 or 300°C before and after 900°C, 15 min annealing. Doses are indicated in the figures.

is observed above and below this amorphous layer, resulting in dislocation formation during the anneal at 900°C. XTEM of the sample after the  $3 \times 10^{13}$  In/cm<sup>2</sup> RT implant shows a damaged crystalline region, in agreement with the RBS measurement. Annealing of this structure also results in dislocation formation. XTEM after annealing of the sample implanted at 300°C with  $3 \times 10^{14}$  In/cm<sup>2</sup> shows the formation of a dislocation network near  $R_p$ , along with several small precipitates (Fig. 13). These dislocations are identified as pre-amorphization damage and are much larger and more complicated than the EOR-loops observed for the RT implant. Thus, suppressing amorphization by implanting at higher temperatures can indeed result in the formation of pre-amorphization damage. The micrograph of the as-implanted structure for the In dose of  $6 \times 10^{13}$  /cm<sup>2</sup> shows the presence of crystal damage, which again gives rise to dislocation formation during the furnace anneal. If the In dose is lowered to  $3 \times 10^{13}$  /cm<sup>2</sup>, crystal damage is still observed. However, no dislocations remain after the anneal of this sample, which is in contrast with the RT implant. The amount of crystal damage for the 300°C implant must have decreased to such a value that stable dislocations could not form during annealing.

A reduction in dislocation formation was observed for the 1 MeV In implants at elevated temperature (section 3.2). In this section, it was shown that elevated temperature implants of 150 keV In for moderate doses can also reduce or suppress dislocation formation. However, for higher doses, increasing the implant temperature changes the secondary damage from the simple EOR-loops to a complicated dislocation network.

## **5. EOR-LOOP FORMATION FOR Ge IMPLANTED AT RT AND LN<sub>2</sub>**

Pre-amorphization damage is avoided if the amount of crystal damage generated by the implant is below a critical value. Annealing an amorphous layer results in the formation of EOR-loops from agglomeration of Si interstitials which are positioned in the a/c transition region. If the amount of crystal damage in the transition region is also reduced below a critical value by performing implants at low temperature, EOR-loop formation may be avoided. To investigate this, amorphizing implants of Ge were performed at RT and LN<sub>2</sub>.

Figure 14 presents RBS measurements of samples implanted with 75 keV <sup>73</sup>Ge for different doses and implant temperatures. A surface amorphous layer with a thickness of 100 nm is obtained for a  $5 \times 10^{14}$  /cm<sup>2</sup> RT implant. For a lower dose ( $4 \times 10^{14}$  /cm<sup>2</sup>) implant at LN<sub>2</sub>, the amorphous layer is almost as thick (90 nm). The Ge implanted structures were annealed at 400°C for 1 hr to avoid the formation of

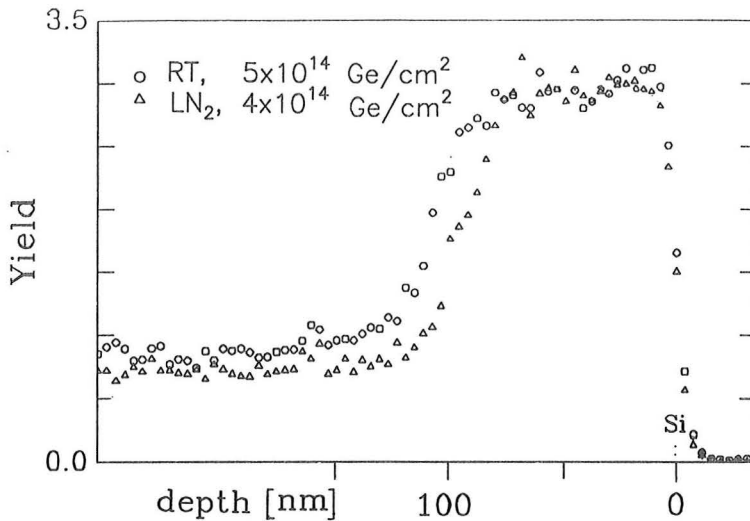


Fig. 14. RBS spectra before annealing of Si implanted with 75 keV Ge. The RT implanted sample received a dose of  $5 \times 10^{14} / \text{cm}^2$  whereas the LN<sub>2</sub> implanted sample a dose of  $4 \times 10^{14} / \text{cm}^2$ .

hairpin dislocations [6], at 600°C for 1 hr to induce regrowth of the amorphous layer, and at 900°C for 15 min to anneal any remaining crystalline damage.

Cross-section and plan-view TEM micrographs of the annealed samples are presented in Fig. 15. A band of EOR-loops at a depth of 100 nm is observed for the RT implant. The diameter of these loops is ~25 nm and their concentration is  $\sim 1 \times 10^{10} / \text{cm}^2$ . In sharp contrast, no dislocations are observed for the LN<sub>2</sub> implant. This means that the concentration of dislocations is lower than  $1 \times 10^5 / \text{cm}^2$ , the detection limit for dislocations in plan-view TEM in our microscope.

The LN<sub>2</sub> implanted sample was also directly annealed at 900°C for 15 min. This anneal was, as for each anneal described in this chapter, performed in a vacuum furnace where it takes some time for the sample to reach the final temperature. Hence, the amorphous layer will have regrown before the end temperature of 900°C is reached. TEM analysis again shows no dislocations, so performing the one step anneal at 900°C was sufficient.

Elimination of EOR-loops was observed for the Ge implanted samples if the implant was performed at LN<sub>2</sub>. It is known that Si amorphizes more readily if the implant is performed at low temperatures and the amorphous layer will be thicker for the same implanted dose [8,12]. This thickness increase results in a lower amount of crystal damage beyond the a/c interface [12,13]. The amount of crystal

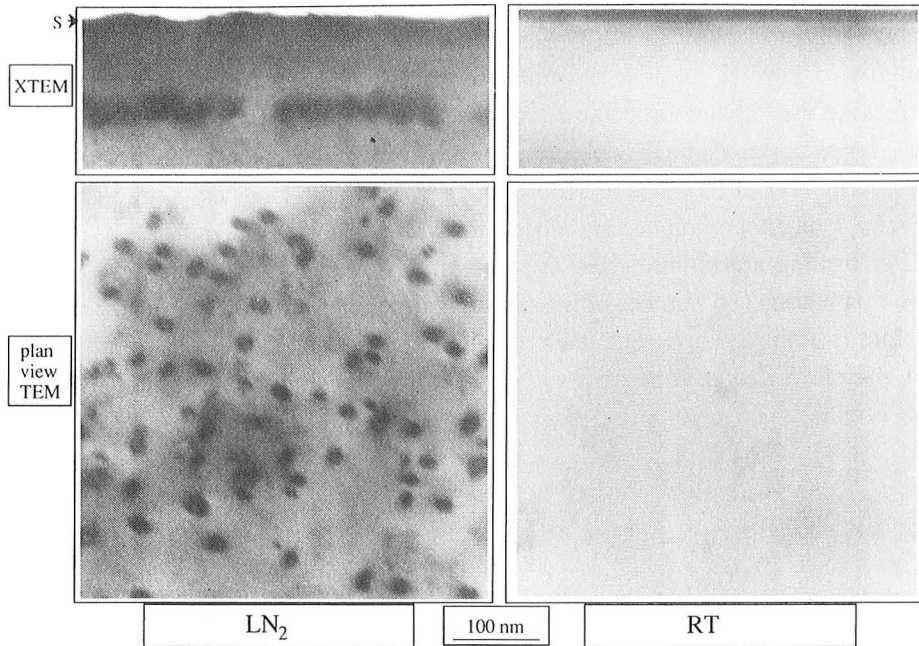


Fig. 15. XTEM and plan-view TEM of Si implanted with 75 keV Ge after 900°C annealing for 15 min. The RT implanted sample received a dose of  $5 \times 10^{14}$  /cm<sup>2</sup> and the LN<sub>2</sub> implanted sample a dose of  $4 \times 10^{14}$  /cm<sup>2</sup>.

damage remaining after the LN<sub>2</sub> implant must have been smaller than the amount needed for dislocation formation.

## 6. CONCLUSIONS

The formation of pre-amorphization damage was investigated for B and In implants. For B implants, the only number which counts for dislocation formation is the total number of Si atoms displaced during the implant. The structure of defect complexes formed during implantation (the primary damage), which is altered by changing the implant temperature or the current density, is not so critical. In the case of In implants, where a-zones are a major part of the primary damage, the critical number of displaced Si atoms needed for dislocation formation decreases by a factor of ~40 with increasing substrate temperature. For implants done above 300°C, the critical number is  $\sim 10^{16}$  /cm<sup>2</sup>, close to the number found for B implants

for which no a-zones are created. The elevated temperature implants not only affect the formation of amorphous Si but also the point defect population.

Implants of 150 keV In at RT result in complete amorphization before the critical amount of crystal damage is reached, so EOR-loops form after annealing. Increasing the implant temperature suppresses amorphization, and the formation of pre-amorphization damage is observed. If the implant dose is lowered, a sub-critical amount of crystal damage,  $< 10^{16}$  displaced Si atoms/cm<sup>2</sup>, is generated for the elevated temperature implant and dislocation formation is avoided.

Performing amorphizing Ge implants at LN<sub>2</sub> instead of RT suppresses EOR loop formation. The number of interstitials in the a/c transition region for the LN<sub>2</sub> implant is probably lower than the critical number needed for dislocation formation and, therefore, dislocations are not observed after high temperature annealing of the LN<sub>2</sub> implant.

## REFERENCES

- [1] F.F. Morehead and B.L. Crowder, *Radiat. Eff.* **6**, 27 (1970).
- [2] H.J. Stein, F.L. Vook, and J.A. Borders, *Appl. Phys. Lett.* **14**, 328 (1969).
- [3] Y-H Lee, N.N. Gerasimenko, and J.W. Corbett, *Phys. Rev. B* **14**, 4506 (1976).
- [4] M.O. Ruault, J. Chaumont, and H. Bernas, *Nucl. Instr. and Meth.* **209/210**, 351 (1983).
- [5] R.J. Schreutelkamp, J.S. Custer, J.R. Liefting, W.X. Lu, and F.W. Saris, *Mater. Sci. Rept.* **6**, 275 (1991).
- [6] K.S. Jones, S. Prussin, and E.R. Weber, *Appl. Phys. A* **45**, 1 (1988).
- [7] P.J. Schultz, C. Jagadish, M.C. Ridgway, R.G. Elliman, and J.S. Williams, *Phys. Rev. B* **44**, 9118 (1991).
- [8] J.S. Williams, *Mat. Res. Soc. Symp. Proc.* **51**, 83 (1985).
- [9] R.S. Nelson, in: *Proceedings European Conference on Ion Implantation*, Reading, England, p. 212 (1970).
- [10] K.S. Jones and D. Venables *J. Appl. Phys.* **69**, 2931 (1991).
- [11] E. Ganin and A. Marwick, *Mat. Res. Soc. Symp. Proc.* **147**, 13 (1989).
- [12] T. Suzuki, H. Yamaguchi, S. Ohzono, and N. Natsuaki, *Ext. Abstr. Int. Conf. on Solid State Dev. and Mat.*, 1163 (1990).
- [13] K. Shoji, A. Fukami, T. Nagano, T. Tokuyama, and C.Y. Yang, *Appl. Phys. Lett.* **60**, 451 (1992).
- [14] M. Servidori and I. Vecchi, *Solid-State Electron.* **24**, 329 (1981).

- [15] W.-K. Chu, J.W. Mayer, and M.-A. Nicolet, *Backscattering Spectrometry* (Academic Press, New York, 1978).
- [16] L.M. Howe and M.H. Rainville, *Nucl. Instr. and Meth.* **B19/20**, 61 (1987).
- [17] S.T. Picraux, J.E. Westland, J.W. Mayer, R.R. Hart, and O.J. Marsh, *Appl. Phys. Lett.* **14**, 7 (1969).
- [18] D.K. Sadana, J. Washburn, P.F. Byrne, and N.W. Cheung, *Mat. Res. Soc. Symp. Proc.* **14**, 511 (1983).
- [19] J. Narayan, O.W. Holland, and B.R. Appleton, *J. Vac. Sci. Technol. B* **1**, 871 (1983).
- [20] J.R. Liefing, J.S. Custer, R.J. Schreutelkamp, and F.W. Saris, to be published in: *Proceedings International School of Materials Science and Technology*, Erice (1991).



## CHAPTER 3

---

### AVOIDING DISLOCATION FORMATION FOR B, P, AND As IMPLANTS IN SILICON

*Implants of B, P, and As in Si lead to dislocation formation after 900 °C annealing if a critical amount of implant damage is exceeded. However, it is possible to implant higher doses without forming dislocations if the dose is implanted in several sub-critical steps. Annealing between each step removes the (sub-critical) implant damage and dislocations do not form. Such avoidance of dislocation formation is demonstrated for 80 keV implants of B and MeV implants of B, P, and As.*

## 1. INTRODUCTION

Ion implantation is one of the key techniques in the semiconductor industry for doping of Si. The great disadvantage of the technique is that damage is created during an implant. Most of this damage can be annealed out, but secondary defects (dislocations) will remain if the as-implanted damage was above a critical level [1]. These defects can have detrimental effects on device performances and should therefore be avoided [2]. Hence, much research is carried out to find ways to reduce the number or the influence of the secondary defects. This research involves hot implantations to inhibit dislocation formation [3] and the formation of buried layers by MeV implants which can act as a gettering layer for microdefects [2,4]. An elegant way to avoid dislocation formation is to perform repetitive implant/anneal steps, where each implant step generates a sub-critical amount of damage. So far, the latter was only shown for MeV implants of In ions in Si [5]. In this chapter we will apply the implant/anneal sequence for the more common dopants like B, P, and As. TEM analysis of MeV and keV single step implants will show dislocation formation after annealing at 900°C for 15 min. Multiple step implants, however, result in dislocation-free material.

## 2. EXPERIMENTAL

Room temperature implants of 1 MeV B, P, and As, and 80 keV B were done in a random direction in Si(100). A current density lower than 20 nA/cm<sup>2</sup> on target was used to avoid beam heating effects. Before annealing, the damage in the Si was measured using 2 MeV He<sup>+</sup> Rutherford backscattering spectrometry (RBS) in the channeling configuration. The implanted samples were annealed in a vacuum furnace (base pressure  $\approx 10^{-7}$  Torr) at 900°C. Cross-section (XTEM) and plan-view transmission electron microscopy were carried out in bright field mode along [011] and [220] direction, respectively. Spreading resistance measurements were performed on bevelled samples with an angle of 0.52° and a depth step of 0.05  $\mu\text{m}$ .

## 3. RESULTS AND DISCUSSION

Three samples were implanted with 1 MeV P to a total dose of  $1.1 \times 10^{14}$  /cm<sup>2</sup> using different implant/anneal sequences. The dose was implanted in a single step, followed by an anneal at 900°C for 15 min, for the first sample. The second sample

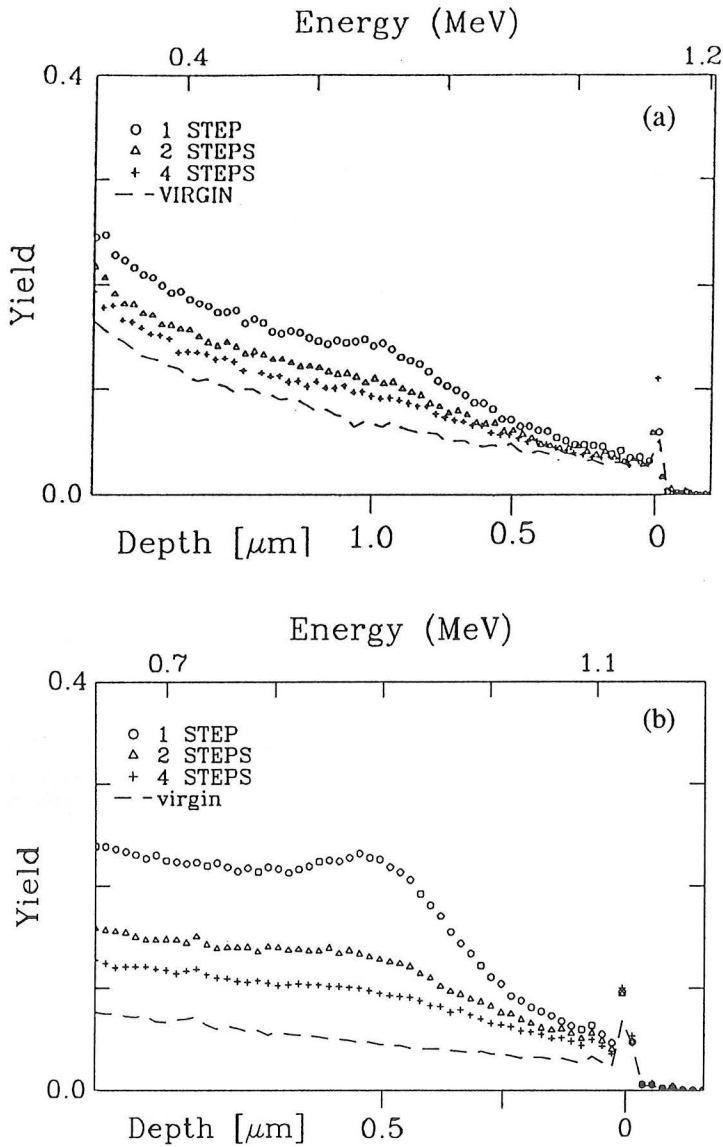


Fig. 1. RBS channeling spectra of 1 MeV, multiple step implanted samples for total doses of (a)  $1.1 \times 10^{14}$  P/cm<sup>2</sup>, and (b)  $8 \times 10^{13}$  As/cm<sup>2</sup>. The total dose for the 4 step implant was reached in 4 steps, where an anneal at 900°C for 15 min was performed after each step.

was implanted in two  $5.6 \times 10^{13}$  P/cm<sup>2</sup> implant steps each followed by the anneal. A third sample was formed by four  $2.8 \times 10^{13}$  P/cm<sup>2</sup> implants each followed by the 15 min, 900°C anneal. RBS channeling spectra, showing the damage levels in the three samples, were taken before the last anneal, see Fig. 1a. The damage peaks at a

depth of  $\sim 1 \mu\text{m}$ . The different damage levels can be converted to a number of displaced Si atoms using the method of Chu *et al.* [6]. This number decreases from  $1.4 \times 10^{17}$  to  $4.7 \times 10^{16} / \text{cm}^2$  as the number of implant steps increases from 1 to 4, see Table I. Schreutelkamp *et al.* have shown that dislocation formation depends critically on the number of displaced Si atoms [1]. For 1 MeV P implants the results from Ref. 1 are also included in table I. From these it is clear that for the 4 step implant and anneal sequence, the number of displaced Si atoms remains below the critical number. Implants of 1 MeV As to a total dose of  $8 \times 10^{13} / \text{cm}^2$  were also performed in 1, 2, and 4 steps. The sequential dose for the 2 step implant was  $4 \times 10^{13} \text{ As/cm}^2$  and for the 4 step implant  $2 \times 10^{13} \text{ As/cm}^2$ . RBS channeling spectra for the three samples, measured before the final anneal, are shown in Fig. 1b. The damage created by the implant peaks at a depth of  $\sim 0.55 \mu\text{m}$ . The number of

TABLE I.

Implant and anneal procedures for P, As, and B implants, along with the number of displaced Si atoms determined with RBS channeling analysis and information concerning dislocation formation (- no dislocations, + dislocations).

SAMPLE	IMPLANT AND ANNEAL SCHEDULE	DISPLACED SILICON ATOMS BEFORE FINAL ANNEAL	DISLOCATIONS OBSERVED
1 MeV P	$2.8 \times 10^{13} / \text{cm}^2$ , 900°C/15min.	$4.7 \times 10^{16} / \text{cm}^2$	-*
	$5.6 \times 10^{13} / \text{cm}^2$ , 900°C/15min.	$1.1 \times 10^{17} / \text{cm}^2$	+*
	1 x ( $1.1 \times 10^{14} / \text{cm}^2$ , 900°C/15min.)	$1.4 \times 10^{17} / \text{cm}^2$	+
	2 x ( $5.6 \times 10^{13} / \text{cm}^2$ , 900°C/15min.)	$9.1 \times 10^{16} / \text{cm}^2$	+
1 MeV As	4 x ( $2.8 \times 10^{13} / \text{cm}^2$ , 900°C/15min.)	$4.7 \times 10^{16} / \text{cm}^2$	-
	1 x ( $8 \times 10^{13} / \text{cm}^2$ , 900°C/15min.)	$3.8 \times 10^{17} / \text{cm}^2$	+
	2 x ( $4 \times 10^{13} / \text{cm}^2$ , 900°C/15min.)	$1.8 \times 10^{17} / \text{cm}^2$	+
1 MeV B	4 x ( $2 \times 10^{13} / \text{cm}^2$ , 900°C/15min.)	$1.0 \times 10^{17} / \text{cm}^2$	-
	1 x ( $2 \times 10^{14} / \text{cm}^2$ , 900°C/15min.)	-	+
	2 x ( $1 \times 10^{14} / \text{cm}^2$ , 900°C/15min.)	-	+
80 keV B	5 x ( $4 \times 10^{13} / \text{cm}^2$ , 900°C/15min.)	-	-
	1 x ( $3.2 \times 10^{14} / \text{cm}^2$ , 900°C/20min.)	-	+
	1 x ( $3.2 \times 10^{14} / \text{cm}^2$ , 900°C/80min.)	-	+
	4 x ( $0.8 \times 10^{14} / \text{cm}^2$ , 900°C/20min.)	-	-

[\*] Ref. 1

displaced Si atoms for the three implant schemes, deduced from the RBS channeling measurements, are listed in Table I. Compared to the analysis of Schreutelkamp *et al.* [1], the number of displaced Si atoms remains below the critical number for dislocation formation in case of the 4 step implant.

XTEM micrographs of the 1 MeV  $1.1 \times 10^{14}$  P/cm<sup>2</sup> implanted samples after the final anneal are shown in Fig. 2. Elongated dislocations, with a length of up to 1  $\mu$ m and longer, are observed for the 1 step implant at a depth near 1  $\mu$ m. The 2 step P implanted sample shows a low concentration of (elongated) dislocations. No dislocations are observed after the final anneal if the implant is performed in four  $2.8 \times 10^{13}$  P/cm<sup>2</sup> steps. Hence, each of the implants in the 4 step sequence will have generated a damage level which could be annealed out without the formation of dislocations.

Figure 2 shows also the XTEM results for the  $8 \times 10^{13}$  /cm<sup>2</sup> 1 MeV As implants. A band with a high concentration of perfect and half dislocation loops ( $\phi \approx 40$  nm) is observed for the 1 step implant. The band is positioned near the damage profile peak at a depth of  $\sim 0.55$   $\mu$ m. A lower concentration of mostly prismatic dislocation loops ( $\phi \approx 100$  nm) is observed if the total dose is implanted in two steps of  $4 \times 10^{13}$  As/cm<sup>2</sup>. Dislocation free material results after the final anneal if the implant is performed in four  $2 \times 10^{13}$  As/cm<sup>2</sup> steps, see Fig. 2. Each implant of  $2 \times 10^{13}$  As/cm<sup>2</sup> generates a sub-critical amount of damage which can be annealed out without forming dislocations.

XTEM of three B implanted samples at 1 MeV to a total dose of  $2 \times 10^{14}$  /cm<sup>2</sup> are presented in Fig. 2. The total B dose was implanted in 1, 2, and 5 steps. RBS channeling did not show a clear dechanneling peak and is for that reason not presented. The single step implant gives rise to a band of extended dislocations at a depth of  $\sim 1.5$   $\mu$ m. The 2 step implant, which consisted of consecutive implants of  $1 \times 10^{14}$  B/cm<sup>2</sup>, gives rise to a band of small dislocation rods after annealing. Hence, the damage resulting from an implant of 1 MeV  $1 \times 10^{14}$  B/cm<sup>2</sup> is above the critical level. Finally, XTEM for the 5 step implant does not show the formation of dislocations, see Fig. 2. This is because the damage created in each sequential implant of  $4 \times 10^{13}$  /cm<sup>2</sup> is below the critical level for dislocation formation, see also ref. 1.

So far, all anneals have been performed at 900°C. However, it is known that ion implant damage in silicon can be annealed at much lower temperatures [7]. Hence, a reduction in dislocation formation for the multiple step implants can also be expected if the intermediate anneals, that is all the anneals except the last one, are performed at a lower temperature. We tested this for the 4-step P implant using intermediate anneals at 100 and 700°C, with the final anneal kept at 900°C. XTEM

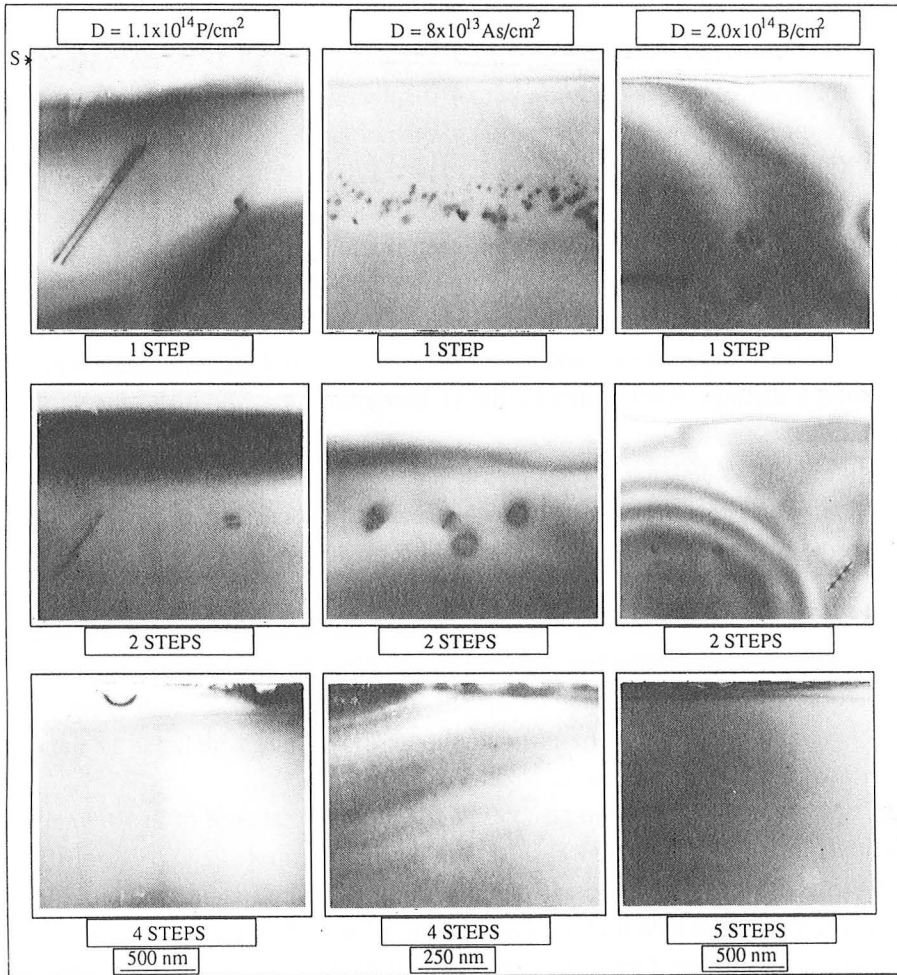


Fig. 2. XTEM analysis of Si implanted with 1 MeV  $1.1 \times 10^{14} \text{ P/cm}^2$ ,  $8 \times 10^{13} \text{ As/cm}^2$ , or  $2 \times 10^{14} \text{ B/cm}^2$ . The number of implant and anneal steps used are denoted in the figure.

analysis for samples subjected to the intermediate anneal of  $100^\circ\text{C}$  for 15 min, see Fig. 3, shows that still elongated dislocations with a length of up to  $1 \mu\text{m}$  are formed. Hence, no large differences are observed compared to the 1 step P implant of Fig. 2. If the intermediate anneal is increased to  $700^\circ\text{C}$ , a significant change in dislocation formation can be noted, see Fig. 3. A high concentration of dislocation rods, with a length of roughly  $0.2 \mu\text{m}$ , is now observed. We postulate that these dislocation rods nucleated and grew in the first three implant/anneal steps. The final anneal at  $900^\circ\text{C}$  dissolved some rods but others grew even further and became large enough to remain after this anneal.

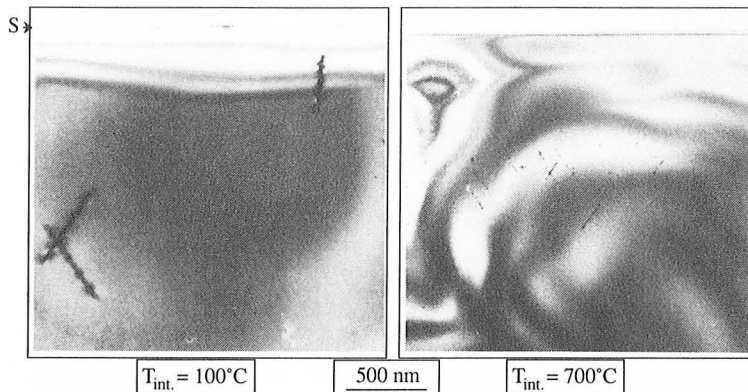


Fig. 3. XTEM of Si implanted with 1 MeV  $1.1 \times 10^{14}$  P/cm<sup>2</sup> in 4 steps. The three anneals after the first three implant steps were performed for 15 min at 100°C or 700°C. The anneal after the last implant step was performed at 900°C for 15 min.

Multiple step implants have also been performed for 80 keV B implants to a total dose of  $3.2 \times 10^{14}$  /cm<sup>2</sup>. Plan-view TEM micrographs of 1 and 4 step implants are presented in Fig. 4. The 1 step implant gives rise to a dislocation density of  $\sim 2 \times 10^9$  /cm<sup>2</sup> after 20 min annealing at 900°C. The size of the dislocations is  $\sim 0.5$   $\mu$ m. The displacement profile for this implant, calculated by TRIM89, peaks at a depth of  $\sim 280$  nm [8]. For that reason it is expected that the dislocations are positioned at a depth of  $\sim 280$  nm. Only one dislocation is observed in the TEM micrograph of the 4 step implant. Hence, the critical damage level for dislocation formation for 80 keV B implants will be reached for a dose of  $\sim 8 \times 10^{13}$  /cm<sup>2</sup>.

The concentration profiles of electrically active B for the multiple step implanted samples, deduced from spreading resistance measurements, are presented in Fig. 5. The profiles peak at a depth of  $\sim 280$  nm. No large differences are observed for the two profiles. Apparently the diffusion of B after 4 implant/anneal steps is not significantly larger than in a single step, but also the activation is not much affected by the presence of dislocations.

The total anneal time for a sample which is implanted in 4 steps is 4 times longer as compared to a sample implanted in 1 step. Therefore we performed plan-view TEM on an 80 keV B sample which was implanted in 1 step and annealed at 900°C for 80 min, see Fig. 4c. If the 80 min annealed sample is compared to the 20 min annealed sample, only small changes in dislocation size and number can be observed (Fig. 4a). Hence, it is clear that the prolonged anneal time does not have a significant influence on dislocation formation.

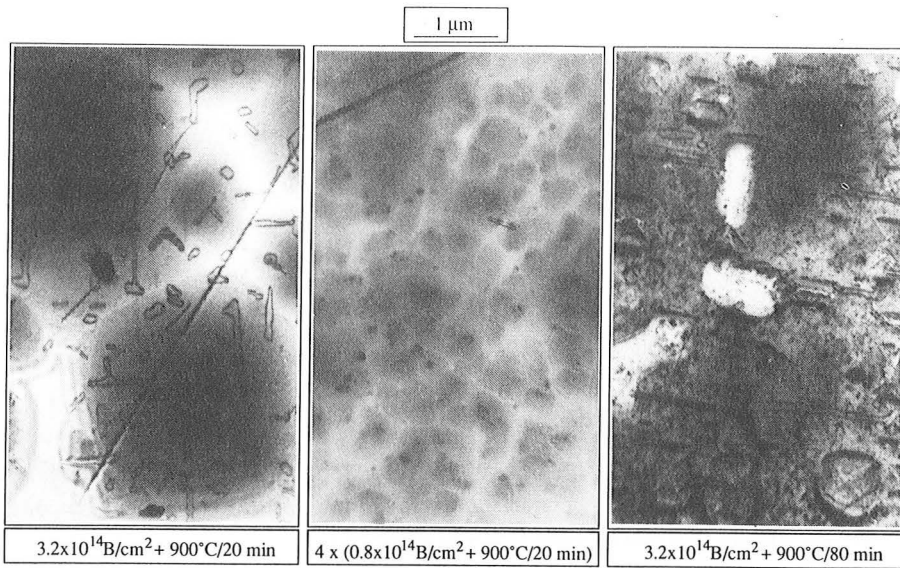


Fig. 4. Plan-view TEM analysis after 900°C annealing of  $3.2 \times 10^{14} / \text{cm}^2$  80 keV B implanted samples. Anneal times and number of steps are denoted in the figure.

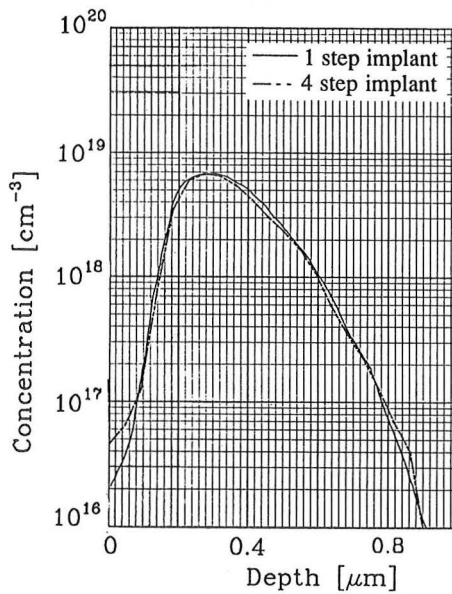


Fig. 5. Electrically active B concentration profiles for Si implanted with  $3.2 \times 10^{14} / \text{cm}^2$  80 keV B in 1 and 4 steps.

#### 4. CONCLUSIONS

Single step implants of B, P, and As result in dislocation formation if more than a critical amount of damage is created during the implant. However, higher doses can be implanted if a sequence of implant and anneal steps is applied, where each implant step generates a sub-critical amount of damage. We have shown this for keV implants of B and MeV implants of B, P, and As.

#### ACKNOWLEDGEMENTS

We would like to thank Corrado Spinella of the institute IMETEM-CNR, Catania for performing the plan-view TEM.

#### REFERENCES

- [1] R.J. Schreutelkamp, J.S. Custer, J.R. Liefting, W.X. Lu, and F.W. Saris, *Mater. Sci. Rept.* **6**, 275 (1991).
- [2] K. Tsukamoto, S. Komori, T. Kuroi, and Y. Akasaka, *Nucl. Instr. and Meth.* **B59/60**, 584 (1991).
- [3] J.R. Liefting, J.S. Custer, R.J. Schreutelkamp, and F.W. Saris, in: *Proceedings International School of Materials Science and Technology*, Erice (1991).
- [4] M. Tamura, T. Ando, and K. Ohyu, *Nucl. Instr. and Meth.* **B59/60**, 572 (1991).
- [5] R.J. Schreutelkamp, J.S. Custer, J.R. Liefting, and F.W. Saris, *Appl. Phys. Lett.* **58**, 2827 (1991).
- [6] W.-K. Chu, J.W. Mayer, and M.-A. Nicolet, *Backscattering Spectrometry*, Academic Press, New York (1978).
- [7] J.W. Corbett, J.P. Karins, and T.Y. Tan, *Nucl. Instr. and Meth.* **B182/183**, 457 (1981).
- [8] J.P. Biersack, and L.G. Haggmark, *Nucl. Instr. and Meth.* **174**, 257 (1980).



## CHAPTER 4

---

### CARBON IMPLANTATION FOR SUPPRESSION OF DISLOCATION FORMATION

*This chapter will show that annealing of Si implanted with moderate doses of 725 keV B results in the formation of secondary defects, the so-called category I dislocations. Surprisingly,  $^{12}\text{C}$ , with roughly the same mass as  $^{11}\text{B}$ , behaves in a very different way. Annealing C implant damage does not result in dislocation formation even for doses > 100 times higher than that required for B implants. C is also able to suppress dislocation formation for co-implanted B ions. The C dose needed to avoid dislocation formation for the B implant increases nonlinearly with B dose. Special C-related secondary defects remain after annealing if the C dose is higher than  $4 \times 10^{15} \text{ /cm}^2$ .*

## 1. INTRODUCTION

Defects in ion implanted silicon have been studied extensively during the last decades. It has been recognized that all types of secondary defects can be put in 5 categories [1]. The first category describes the formation of dislocations in Si for implants below the amorphization threshold. These dislocations result from agglomeration of Si interstitials during high temperature annealing if a minimum amount of implant damage has been generated [2]. This criterion for dislocation formation has been demonstrated for many elements of the periodic table. For example, the critical damage level for an 1 MeV B implant is reached for a dose between  $4$  and  $10 \times 10^{13}$  /cm<sup>2</sup>, if the anneal is performed at 900°C for 15 min [2]. On the other hand, for C implants it was found that dislocations do not form [3]. There, it was suggested that dislocation formation did not occur because the small C atom acts as a sink for the excess Si self-interstitials, leaving too few Si interstitials for dislocation formation. However, this was shown for ion doses of  $1 \times 10^{16}$  /cm<sup>2</sup> and anneal temperatures as high as 1000°C [3]. Other groups have shown that dislocation formation resulting from P implants, can be suppressed to a large extent by additional C implants [4]. In that case, it was assumed that C also traps the Si interstitials generated by the P implant. However, this was investigated only for a P dose of  $1 \times 10^{15}$  /cm<sup>2</sup>. In this chapter we compare dislocation formation for 725 keV B implants of doses between  $6 \times 10^{13}$  and  $4 \times 10^{15}$  /cm<sup>2</sup> and 800 keV C implants for doses ranging from  $2 \times 10^{14}$  to  $1 \times 10^{16}$  /cm<sup>2</sup> by Rutherford backscattering spectrometry (RBS) and cross-section transmission electron microscopy (XTEM). Combined C and B implants have been studied to see whether or not an additional C implant can reduce the number of secondary defects due to the B implant. The necessary C dose to avoid dislocation formation for different B doses will be given.

## 2. EXPERIMENTAL

Room temperature implants of 725 keV B and 800 keV C were done in 5-15 Ωcm, p-type float zone Si (100) in a random direction. In the case of the combined C and B implants, the C was implanted first. A current density lower than 30 nA/cm<sup>2</sup> on target was used. The implant damage in the Si was measured using 2 MeV He<sup>+</sup> Rutherford backscattering spectrometry (RBS) in the channeling configuration. After the last implant, the samples were annealed in a vacuum furnace (base pressure  $\approx 10^{-7}$  Torr) at 900°C for 15 min. Cross-section transmission electron microscopy (XTEM) was carried out in bright field with the electron beam along [011].

### 3. RESULTS

Figure 1 shows RBS spectra of samples implanted with 725 keV  $^{11}\text{B}$  for doses of  $5 \times 10^{14}$ ,  $1 \times 10^{15}$ , and  $4 \times 10^{15}$  / $\text{cm}^2$ . The displacement profile peaks at a depth of  $\sim 1.3 \mu\text{m}$  and increases with dose. The B dose of  $5 \times 10^{14}$  / $\text{cm}^2$  generates a damage profile containing  $\sim 2 \times 10^{17}$  / $\text{cm}^2$  displaced Si atoms, which is far more than the critical number for dislocation formation for B implants [2]. Therefore dislocation formation is expected. Figure 1b shows RBS channeling spectra of the B implanted

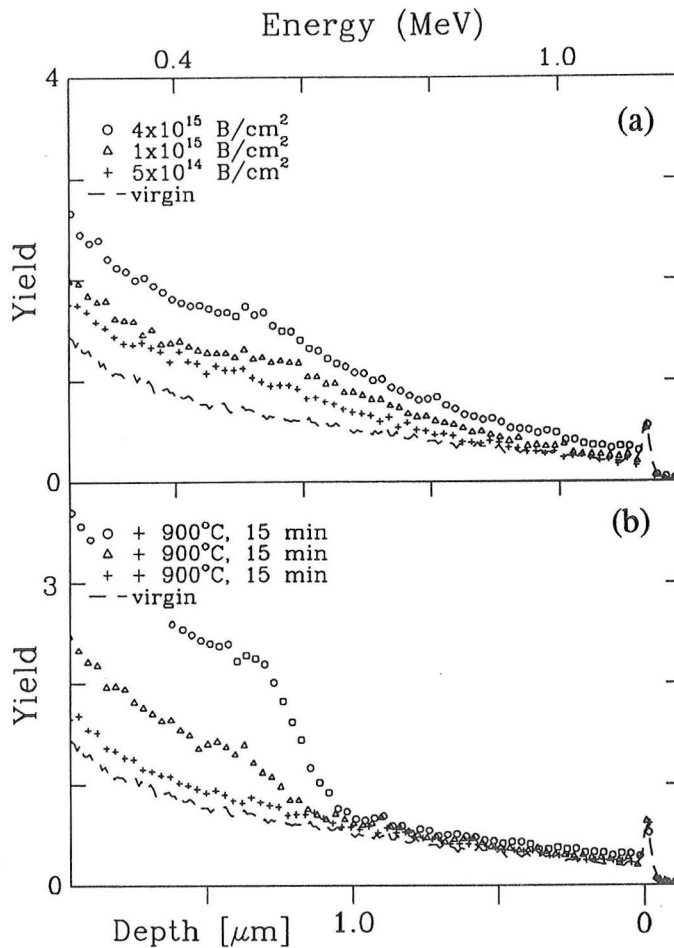


Fig. 1. RBS channeling measurements of Si implanted with 725 keV B, before (a) and after (b)  $900^\circ\text{C}$ , 15 min annealing. The increase in dechanneling at a depth of  $1.2 \mu\text{m}$  for the annealed samples indicates the presence of dislocations.

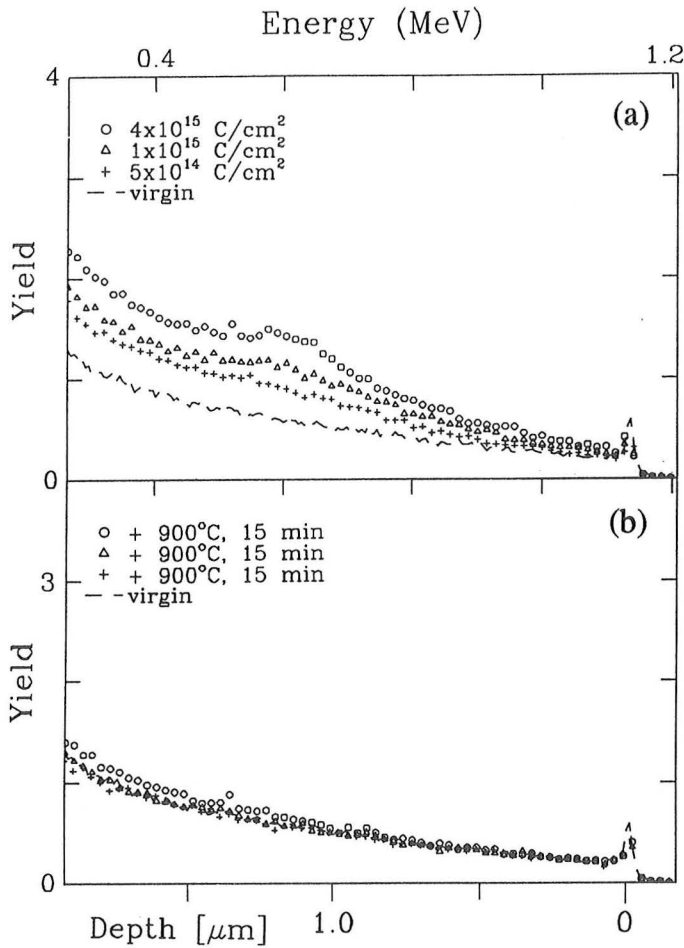


Fig. 2. RBS channeling measurements of Si implanted with 800 keV C, before (a) and after (b) 900°C, 15 min annealing. No strong increase in dechanneling is observed for the annealed samples.

samples after annealing for 15 min at 900°C. A strong increase in dechanneling at a depth of  $\sim 1.2 \mu\text{m}$  is observed for all three B doses. We attribute this increase in dechanneling to the presence of dislocations. The rise in dechanneling is strongest for the highest B dose, indicating that dislocation formation is most severe for this dose.

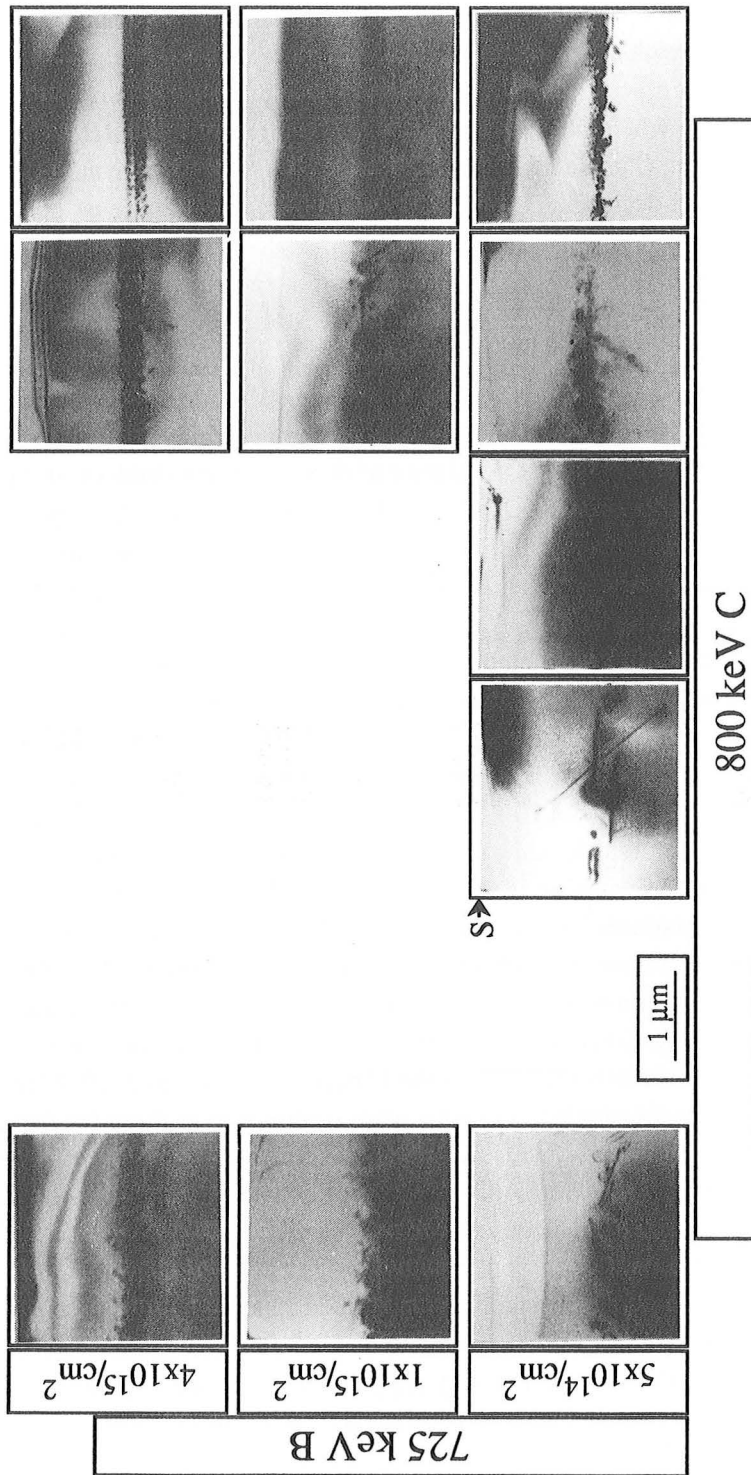
Implants of 800 keV <sup>12</sup>C were also performed to doses of  $5 \times 10^{14}$ ,  $1 \times 10^{15}$ , and  $4 \times 10^{15}$  /cm<sup>2</sup>. This implant energy is higher than used for the B implant to compensate for the higher stopping for the slightly heavier C atoms. Figure 2a

shows RBS spectra of the C implanted samples before annealing. The dechanneling increases with dose. For a dose of  $5 \times 10^{14} / \text{cm}^2$ , the damage profile peaks at a depth of  $\sim 1.1 \mu\text{m}$  and contains  $\sim 2 \times 10^{17} / \text{cm}^2$  displaced Si atoms. Hence, dislocation formation would normally be expected. Figure 2b shows RBS channeling spectra of the three C implanted samples after annealing for 15 min at  $900^\circ\text{C}$ . Only a small increase in dechanneling is observed for the highest C dose of  $4 \times 10^{15} / \text{cm}^2$ , which is in contrast with the results for the B implanted sample. The spectra for the C doses of  $5 \times 10^{14}$  and  $1 \times 10^{15} / \text{cm}^2$  could not even be distinguished from that of an unimplanted sample. Hence, from RBS we conclude that secondary defect formation for C and B implants is completely different.

XTEM micrographs of B, and combined B *and* C implanted samples are presented in Fig. 3. The left most column displays micrographs of samples implanted with B only. One elongated dislocation at a depth of  $\sim 1.2 \mu\text{m}$  is observed for a single B dose of  $6 \times 10^{13} / \text{cm}^2$ . Hence, this dose must have generated a damage level just above the critical level for dislocation formation. The density of dislocations is increasing, finally resulting in a dislocation network, if the B dose is raised to  $1 \times 10^{15} / \text{cm}^2$ . A dose of  $4 \times 10^{15} \text{ B/cm}^2$  results in an even more dense dislocation network. Hence, the XTEM data confirm the results of the RBS measurements in Fig. 1, which suggested that dislocations form for B implants.

The bottom row in Fig. 3 shows XTEM of a B implant of  $6 \times 10^{13} / \text{cm}^2$  combined with C implants for increasing dose. No dislocations are observed in the micrograph for the  $6 \times 10^{13} \text{ B/cm}^2$  *and*  $2 \times 10^{14} \text{ C/cm}^2$  implanted sample. Hence, this extra C implant is able to suppress dislocation formation of the B implant. Dislocation formation is still suppressed if the C dose is raised to  $4 \times 10^{15} \text{ C/cm}^2$ . The micrograph for the C dose of  $4 \times 10^{15} / \text{cm}^2$  shows a shady band and some special, unknown type of secondary defects, first observed by Skorupa *et al.* [5]. High resolution or dark field microscopy could not clarify the character of the shady band or the C-related secondary defects [5,6]. The concentration of C-related secondary defects increased if the C dose was raised to  $1 \times 10^{16} / \text{cm}^2$ . The XTEM results for the single C implants were comparable to those for the samples which were also implanted with  $6 \times 10^{13} \text{ B/cm}^2$ , and are therefore not shown. Hence, the RBS data for the single C implants presented in Fig. 2, suggesting that a low concentration of defects could be observed for a dose of  $4 \times 10^{15} / \text{cm}^2$  only, is confirmed by XTEM.

An increase in the number of elongated dislocations was observed for a single B implant if the dose was raised to  $1 \times 10^{14} / \text{cm}^2$ . Fig. 3 shows that dislocation formation can only be partially suppressed if an extra implant of  $2 \times 10^{14} \text{ C/cm}^2$  is performed. Dislocations are eliminated if the C dose is raised to  $5 \times 10^{14} / \text{cm}^2$ . The



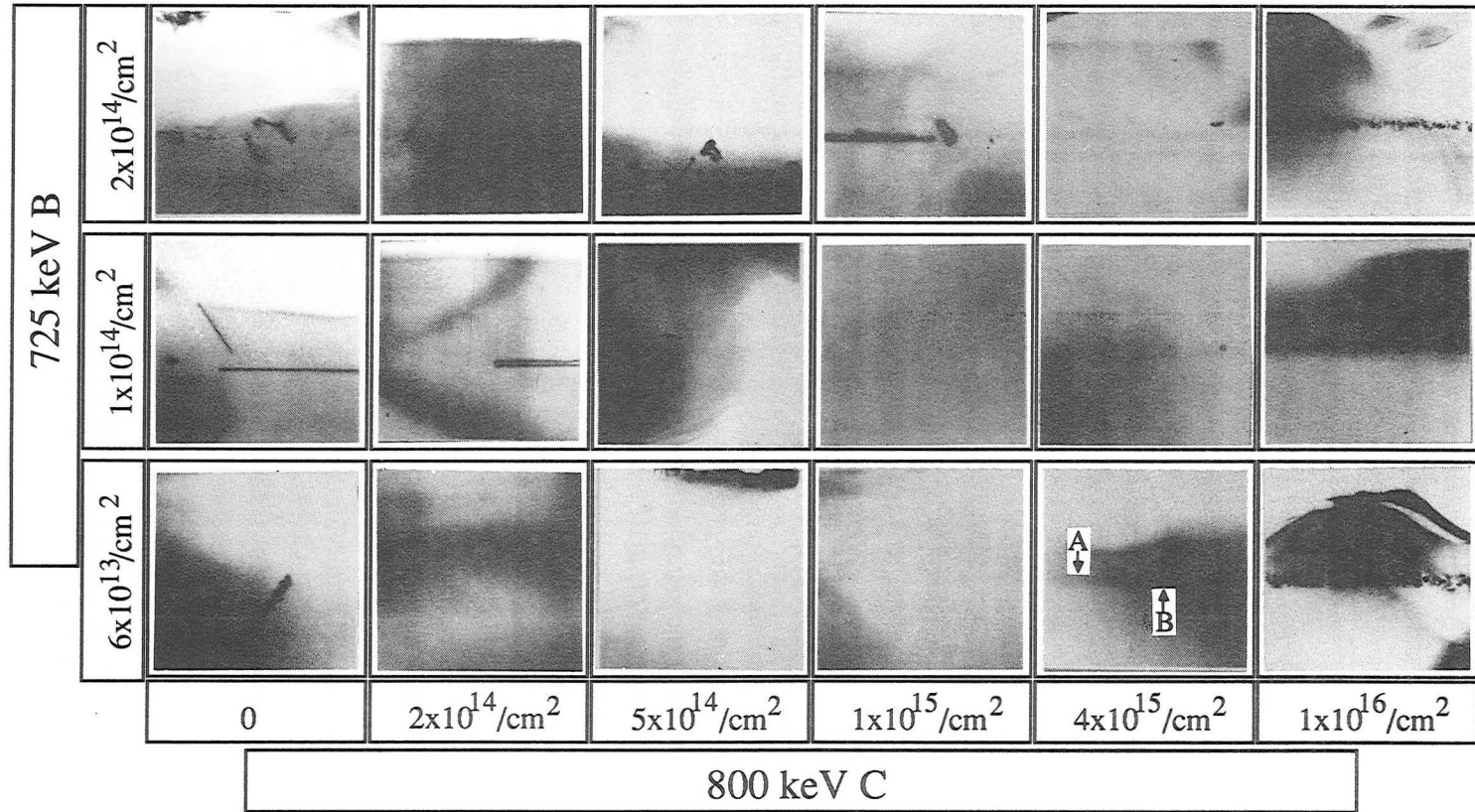


Fig. 3. XTEM results after annealing for combined 725 keV B and 800 keV C implants. Implant doses for B and C are indicated. The shady band is denoted by an 'A' and the C-related secondary defects by a 'B', discussed in the text.

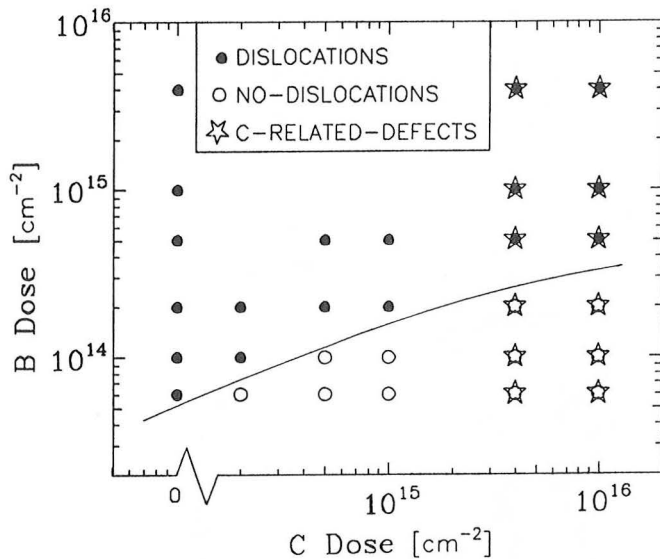


Fig. 4. Summary of the XTEM results for the 725 keV B and 800 keV C implants. The full drawn line gives the necessary C dose if dislocation formation has to be avoided.

special type of C-related secondary defects are again seen for an extra implant of  $4 \times 10^{15}$  C/cm<sup>2</sup>. The B dose of  $2 \times 10^{14}$  /cm<sup>2</sup> results in an increased number of dislocations, which is apparently not influenced by extra C implants of a dose up to  $5 \times 10^{14}$  /cm<sup>2</sup>. A C dose of  $1 \times 10^{15}$  /cm<sup>2</sup> seems to reduce the number of dislocations whereas a dose of  $4 \times 10^{15}$  /cm<sup>2</sup> is sufficient to suppress them completely. Single implants with  $5 \times 10^{14}$ ,  $1 \times 10^{15}$ , and  $4 \times 10^{15}$  /cm<sup>2</sup> B show a further increase in dislocation formation. Extra C implants cannot suppress dislocation formation any more for these high B doses, although a C dose of  $1 \times 10^{16}$  /cm<sup>2</sup> is able to limit B induced dislocation formation to the substrate side, Fig. 3.

A summary of the XTEM results for the combined B and C implants is shown in Fig. 4. The figure shows that dislocation formation for a B dose of  $6 \times 10^{13}$  /cm<sup>2</sup> can be avoided by extra C implants for doses as low as  $2 \times 10^{14}$  /cm<sup>2</sup>, which is  $\sim 3$  times the B dose. If the B dose is raised to  $1 \times 10^{14}$  /cm<sup>2</sup>, the C dose has to be raised to roughly  $5 \times 10^{14}$  /cm<sup>2</sup>, which is 5 times higher. Finally, for a B dose of  $2 \times 10^{14}$  /cm<sup>2</sup>, a 20 times higher C dose has to be implanted if dislocation formation has to be avoided. For the high-dose combined B and C implants, both dislocations and C-related secondary defects remain after annealing.

#### 4. DISCUSSION AND CONCLUSIONS

Dislocations are formed after 900°C annealing for 15 min if a minimum amount of implant damage has been generated [2]. This amount of damage is produced by a 725 keV  $^{11}\text{B}$  implant to a dose of  $6 \times 10^{13} / \text{cm}^2$ . Still, it has been recognized for a few years that MeV  $^{12}\text{C}$  implants can be performed for doses  $> 10^{15} / \text{cm}^2$  without the formation of dislocations after annealing at 1000°C. It is shown in this chapter that dislocation formation for C implants is still avoided in case the complete experimental procedure for 725 keV B and 800 keV C implants is comparable. Therefore C is, to our knowledge, the only exception on the criterion for dislocation formation. Wong *et al.* suggested that carbon in silicon is undersized enough to create free volume for carbon/self-interstitial agglomerates, leaving too few interstitials for agglomerating into dislocations [3].

It is possible that C traps not only interstitials of its own implant, but also the interstitials from co-implanted ions. Tamura *et al.* has shown that dislocation formation of 1.5 MeV P to a dose of  $1 \times 10^{15} / \text{cm}^2$  can be largely suppressed by co-implanting 1.15 MeV C to a dose of  $4 \times 10^{15} / \text{cm}^2$  [4]. There it was shown that the reduction in dislocation formation was strongest if the C was overlapping the damage region generated by the P implant. A distance of only 0.2  $\mu\text{m}$  between the C and the damage profile already degraded the influence of the C implant. However, this was for high implant doses. On the other hand, for lower doses Kuroi *et al.* have shown that a 1.6 MeV C implant can getter interstitials generated by a 700 keV,  $1 \times 10^{14} \text{ Si/cm}^2$  implant, where the damage profiles are separated by at a distance of 1.5  $\mu\text{m}$  [7]. Lu *et al.* showed that damage generated by a 2.2 MeV B implant can interact with a damage layer close to the surface created by a Si implant [8]. In these two cases, where the implanted dose is low, interaction seems to be possible over distances of a few microns. In our combined B and C implants, the gettering ability for the C implant seems to be limited to B doses of  $5 \times 10^{14} / \text{cm}^2$  and below. This is somewhat lower compared to the results found for the combined P and C implants. This can be attributed to the  $\sim 0.1 \mu\text{m}$  difference in position of the defect bands for the B and C implants and to the difference in straggling for the B and C implants, which is smaller for the heavier C atoms. Hence, the C profile does not overlap completely with the displacement profile generated by the B implant. Since the communication between the B generated damage and the C will decrease for higher doses, because dislocations form more readily, dislocations will again appear if the B dose gets too high.

**REFERENCES**

- [1] K.S. Jones, S. Prussin, and E.R. Weber, *Appl. Phys. A* **45**, 1 (1988).
- [2] R.J. Schreutelkamp, J.S. Custer, J.R. Liefting, W.X. Lu, and F.W. Saris, *Mater. Sci. Rept.* **6**, 275 (1991).
- [3] H. Wong, N.W. Cheung, P.K. Chu, J. Liu, and J.W. Mayer, *Appl. Phys. Lett.* **52**, 1023 (1988).
- [4] M. Tamura, T. Ando, and K. Ohyu, *Nucl. Instr. and Meth.* **B59/60**, 572 (1991).
- [5] W. Skorupa, R. Kögler, K. Schmalz, and H. Bartsch, *Nucl. Instr. and Meth.* **B55**, 224 (1991).
- [6] N.W. Cheung, private discussion.
- [7] T. Kuroi, S. Komori, K. Fukumoto, Y. Mashiko, K. Tsukamoto, and Y. Akasaka, *Ext. Abstr. Int. Conf. Solid State Devices and Materials*, 56 (1991).
- [8] W.X. Lu, Y.H. Qian, R.H. Tian, Z.L. Wang, R.J. Schreutelkamp, J.R. Liefting, and F.W. Saris, *Appl. Phys. Lett.* **55**, 1838 (1988).





## CHAPTER 5

---

### IMPROVED DEVICE PERFORMANCE BY MULTI STEP OR CARBON CO-IMPLANTS

*High-energy ion implantation is used for forming the collector in vertical bipolar transistors in a BiCMOS process. Secondary defects, remaining after annealing the implant damage, give rise to an increased leakage current and to collector-emitter shorts. These shorts reduce the transistor yield. The use of multiple step implants or the introduction of a C gettering layer are demonstrated to avoid dislocation formation. Experimental results show that these schemes subsequently lower the leakage current and dramatically increase device yield. The presence of C can cause increased collector/substrate leakage, indicating that the C profile needs to be optimized with respect to the doping profiles.*

## 1. INTRODUCTION

High-energy ion implantation is a convenient processing step that offers a high degree of reproducibility. Moreover it enables formation of retrograde n- or p-wells after the high temperature field oxidation step [1,2]. After the LOCOS (LOCAl Oxidation of Silicon) step is done, the tub can be implanted in a self-aligned way, which makes the need for area-consuming stopper implants superfluous. Due to a reduced lateral diffusion of the dopants, high-energy ion implantation results in an increased packing density compared with processes using conventional buried layers [3].

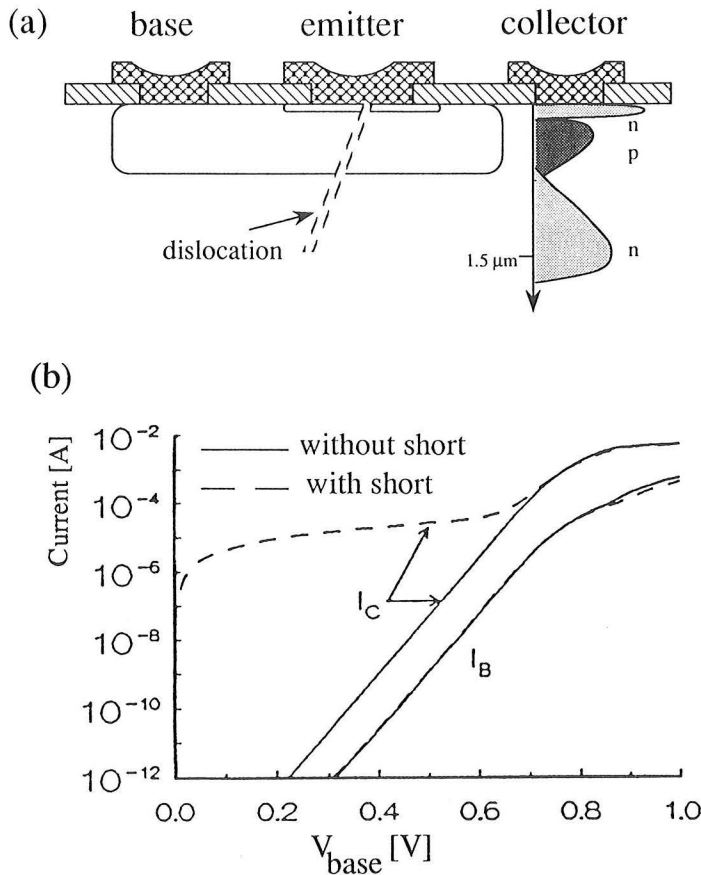


Fig. 1. (a) Schematic of a vertical transistor formed by high-energy ion implantation. The collector implant gives rise to dislocation formation during annealing, which can result in collector-emitter shorts. (b) These shorts give rise to excess collector currents, as is illustrated in the Gummel plot.

Numerous technologies and devices have been realized using high-energy ion implantation. In CMOS processes, the high-energy implanted retrograde well offers a reduced susceptibility to latch-up [4]. In bipolar technology, it can be used to fabricate a pedestal collector to improve the frequency behavior [5] or to simplify processing [3,6]. Other applications of high-energy ion implantation include the realization of vertically integrated DRAM cells [7] or very fast EEPROM cells using a buried injector [8].

The major problem with high-energy implants is the formation of dislocations during annealing [6,9,10]. These dislocations form only if a critical amount of implant damage has been exceeded [11]. This issue applies particularly to the fabrication of collector regions, because the implanted dose must be sufficiently high to obtain a low collector resistance, which gives rise to high damage levels. If the dislocations intersect a junction, an increased leakage current can result. Furthermore, when both the collector/base and the emitter/base junctions are connected via a dislocation, collector-emitter (c-e) shorts may arise by enhanced diffusion of (emitter) dopants along the dislocations (Fig. 1a). This results in a parasitic resistance behavior in the transistor characteristics, as is shown in the Gummel plot of Fig. 1b. In general, these c-e shorts are an important yield problem in bipolar device manufacturing. Although some improvement has been reported by performing extended anneal treatments [6], no structural solution for this problem has been found until now.

Dislocations are not observed if a sub-critical amount of damage is generated by a low dose ( $1 \times 10^{13}$  P/cm<sup>2</sup>) collector implant [11] and no yield problems result [12]. However, a P dose of  $\sim 4 \times 10^{13}$  /cm<sup>2</sup> is needed for an acceptable collector

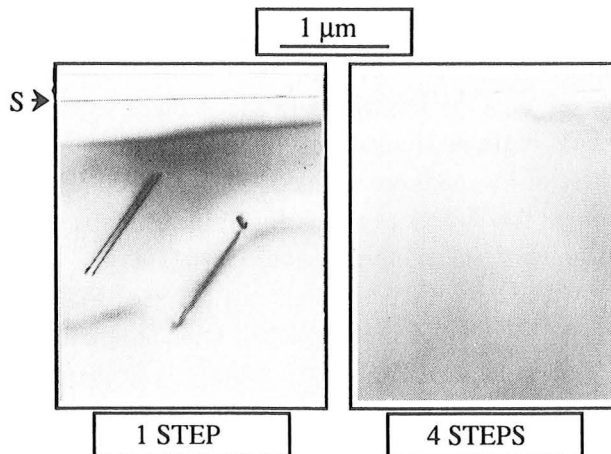


Fig. 2. XTEM analysis of Si implanted with 1 MeV  $1.1 \times 10^{14}$  /cm<sup>2</sup> P in 1-step or 4-steps. An anneal at 900°C for 15 min was performed after each implant step.

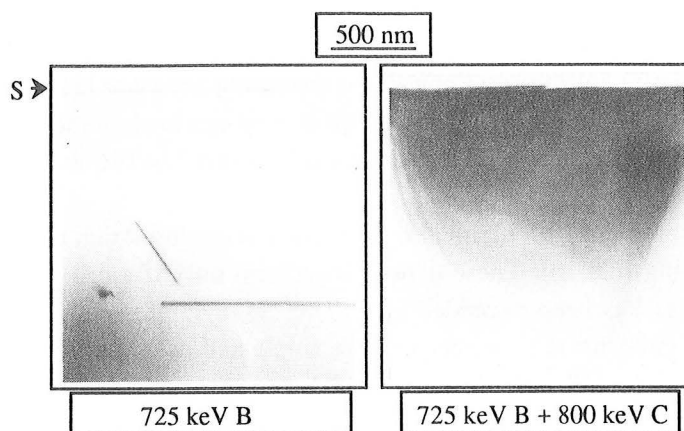


Fig. 3. XTEM analysis of Si implanted with 725 keV  $1 \times 10^{14}$  /cm<sup>2</sup> B without and with an extra 800 keV  $5 \times 10^{14}$  /cm<sup>2</sup> C implant. An anneal at 900°C for 15 min was performed after the implants.

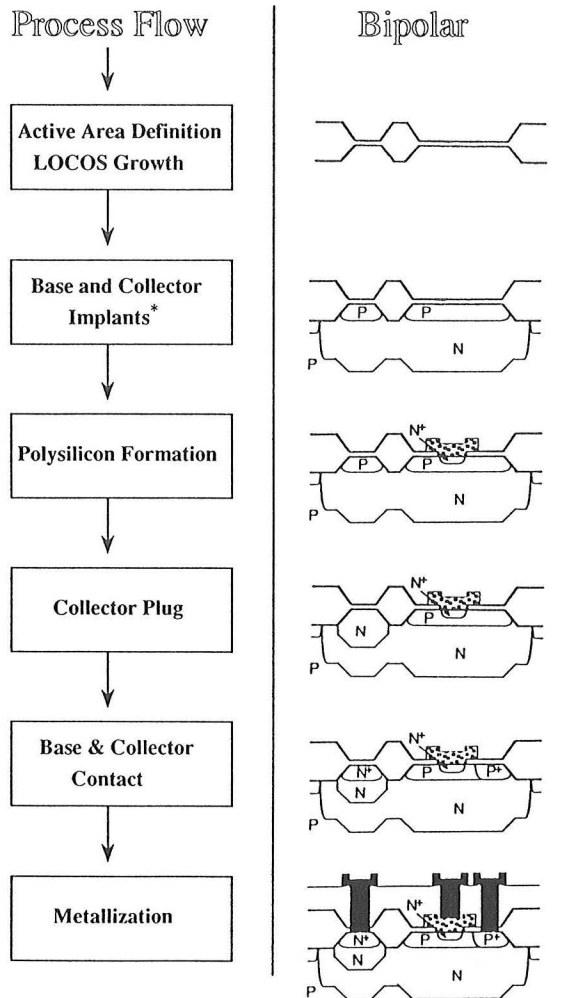
resistance [3], but this dose gives rise to dislocation formation [11] and, subsequently, c-e shorts [12]. In this chapter, two methods are applied to prevent dislocation formation for the higher P dose. The principle of the two methods is explained in the following. In the first method, an implant is performed in multiple steps. Figure 2 shows that annealing a  $1.1 \times 10^{14}$  /cm<sup>2</sup> 1 MeV P implant gives rise to dislocation formation with a density of  $\sim 5 \times 10^8$  /cm<sup>2</sup>. However, if this implant is performed in 4 steps of  $2.8 \times 10^{13}$  /cm<sup>2</sup>, where each step generates a sub-critical amount of damage and is followed by a 900°C, 15 min anneal, no dislocations are observed [11,13,14].

In the second method, C is implanted in the damage region. Annealing a  $1 \times 10^{14}$  /cm<sup>2</sup> 725 keV B single implant results in the formation of dislocations (Fig. 3), whereas these dislocations are avoided if a  $5 \times 10^{14}$  /cm<sup>2</sup> 800 keV C is also implanted. It is thought that C acts as a sink for Si interstitials, thereby avoiding these interstitials to agglomerate and form dislocations [15-17].

This chapter describes how these two methods are used to avoid dislocation formation for the  $4 \times 10^{13}$  P/cm<sup>2</sup> 1.5 MeV collector implant in a BiCMOS process. For the multiple step sequence,  $2 \times (2 \times 10^{13}$  P/cm<sup>2</sup>) is implanted, and for the introduction of a C layer,  $\sim 1.15$  MeV C is implanted to doses of 2 and  $5 \times 10^{14}$  /cm<sup>2</sup>. Electrical measurements on bipolar devices in which the two methods for avoiding dislocation formation have been applied, are presented.

## 2. SAMPLE PREPARATION

For the full BiCMOS device fabrication, three wafers (3-inch, 20 mΩcm, *p*-type) with a 4 μm thick epitaxial layer (10 Ωcm, *p*-type) were used. Figure 4 summarizes process conditions. After growing the field oxide, the tubs for the CMOS devices were implanted. The collector and base of the bipolar devices were formed after fabrication of the CMOS gates. The base was implanted with  $1 \times 10^{13} / \text{cm}^2$  40 keV B. The collector implant,  $4 \times 10^{13} / \text{cm}^2$  1.5 MeV P, was done



\* see also Table I.

Fig. 4. Process flow for forming the bipolar device structures.

Table 1.  
Implants for collector region.

	WAFER 1	WAFER 2	WAFER 3
collector implant	$2 \times (2 \times 10^{13} \text{ P/cm}^2)$	$4 \times 10^{13} \text{ P/cm}^2$	$4 \times 10^{13} \text{ P/cm}^2$
Carbon co-implant (part of the wafer)	-	$2 \times 10^{14} \text{ C/cm}^2$	$5 \times 10^{14} \text{ C/cm}^2$
anneal	$2 \times (900^\circ\text{C}/15 \text{ min})$	$900^\circ\text{C}/15 \text{ min}$	$900^\circ\text{C}/15 \text{ min}$

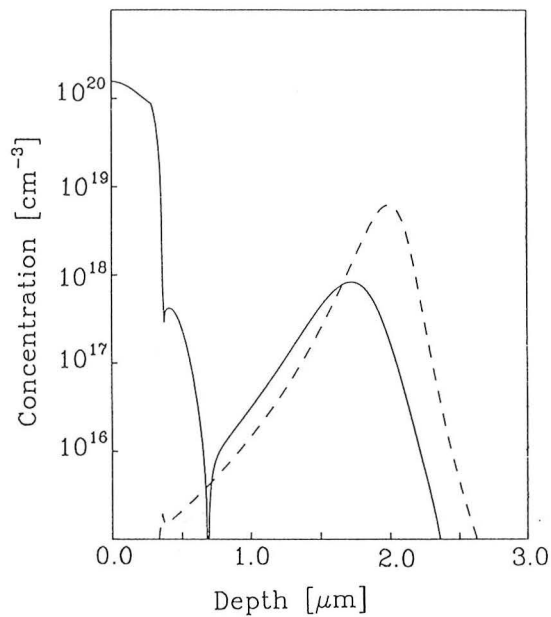


Fig. 5. Doping profile (drawn line) of bipolar transistor co-implanted with  $2 \times 10^{14} \text{ C/cm}^2$  (broken line), as simulated with SUPREM III.

aligned to the  $0.6 \mu\text{m}$  LOCOS oxide, while the LOCOS was covered with a resist layer. The collector of wafer 1 was implanted in two steps of  $2 \times 10^{13} \text{ P/cm}^2$ , with each step followed by a  $900^\circ\text{C}$  anneal for 15 min in  $\text{N}_2$ -ambient. For wafers 2 and 3, after a single  $4 \times 10^{13} \text{ P/cm}^2$  implant, parts of the wafers were co-implanted with 1.15 MeV C to doses of 2 and  $5 \times 10^{14} / \text{cm}^2$ , respectively. These wafers were subsequently annealed at  $900^\circ\text{C}$  for 15 min in  $\text{N}_2$ -ambient. Table I specifies the

collector implant procedures for the three wafers. After annealing, the emitter window was opened in the 25 nm thick screening oxide and a polysilicon emitter was made.

The transistor doping profile co-implanted with  $2 \times 10^{14}$  C/cm<sup>2</sup>, as simulated with SUPREM III, is presented in Fig. 5. The C implant energy is such that dislocation formation for the P implant is avoided most efficiently [15]. The projected range ( $R_p$ ) of C is in that case 0.2  $\mu\text{m}$  deeper than the  $R_p$  of P.

### 3. ELECTRICAL MEASUREMENTS

Bipolar device measurements were performed on transistors of wafers 2 and 3 which were made by the standard process (no C implanted). Some of the Gummel plots for these "standard" transistors showed excessive collector current densities at low base-emitter voltages (Fig. 6). This is attributed to the presence of c-e shorts. The yield of these standard transistors as a function of emitter area is presented in Fig. 7. For cells with an emitter area of  $10^4 \mu\text{m}^2$ , 65% of the emitters are shorted, decreasing to 20% for an area of  $1200 \mu\text{m}^2$ . The larger the area, the higher the probability that at least one dislocation crosses both the base/emitter and collector/base junction. In a first order approximation, the yield is an exponential function of the emitter area, with a "fatal" defect density per unit area of

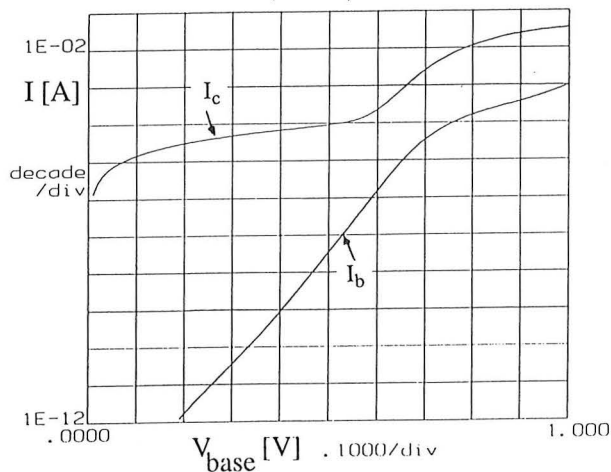


Fig. 6. Gummel plot of transistor with standard collector ( $10^4 \mu\text{m}^2$  emitter). The excessive collector current at low base-emitter voltages is attributed to the presence of c-e shorts.

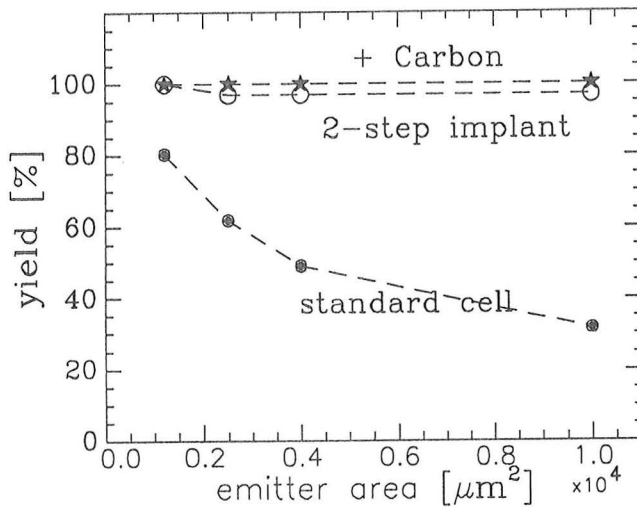


Fig. 7. Yield of bipolar transistors with standard, 2-step implanted and C co-implanted collectors, as a function of emitter area.

$1.25 \times 10^4 / \text{cm}^2$  [18]. This density of defects is in agreement with results found earlier for MeV implanted collector regions, where the dislocation density near the surface was investigated with a Secco-type defect etch [6,9]. Hence, the c-e shorts are likely caused by dislocations running from the collector to the surface region. However, the "fatal" defect density of  $1.25 \times 10^4 / \text{cm}^2$  is more than 4 orders of magnitude smaller than dislocation densities observed for medium dose MeV P implants (see *e.g.* Fig. 2). Hence, only 1 out of  $10^4$  dislocations is fatal, in agreement with results obtained for keV-implanted bipolar transistors [19].

Electrical measurements were also performed on transistors with 2-step implanted collectors and on transistors with C co-implanted collectors. The yield of these transistors as a function of emitter area is presented in Fig. 7. For the multi step implants, only 3% of the transistors with large emitter areas showed the presence of shorts. The smallest emitters ( $1200 \mu\text{m}^2$ ) exhibited no shorts at all. Thus, an enormous improvement in yield is obtained compared to the results for the standard bipolar transistors. For the collectors co-implanted with C, the results were even better. There, none of the transistors showed the excess collector current behavior, independent of emitter area or C-dose (Fig. 7). A typical example of a Gummel plot, where shorts were avoided by either the 2-step implant or the C co-implant, is presented in Fig. 8. The transistor exhibited good characteristics over more than eight decades with a common emitter current gain ( $h_{fe}$ ) of  $\approx 80$ .

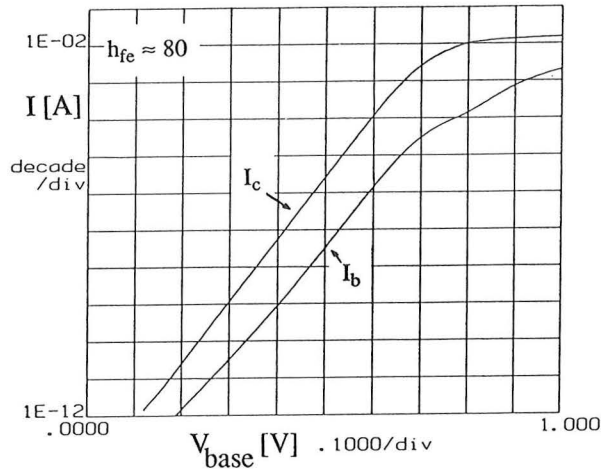


Fig. 8. Gummel plot of transistors with 2-step implanted or C co-implanted collector ( $10^4 \mu\text{m}^2$  emitter).

In addition to fatal shorts, dislocations can also affect junction characteristics such as leakage currents. A defect-free diode has reverse I-V characteristics which can be fitted with a power law  $I \propto V^n$  with  $n \approx 0.5$  [18-20]. For the I-V characteristics of the standard separate collector/base diodes (no emitter formed),  $n$  was  $\sim 1.9$  for lower and  $\sim 4.2$  for higher voltages (Fig. 9). This is normally observed for junctions containing dislocations [19-21]. (The dislocations in the depletion region establish efficient breakdown regions, which give rise to the higher voltage dependence [19].) For the 2-step and for the C co-implanted diodes, the leakage current density decreased by an order of magnitude at 5 V reverse bias.

Here,  $n$  was  $\sim 0.7$  only for lower voltages, indicating an improved, but still not perfect leakage behavior. For the C co-implanted diodes, C-related defects will cause the leakage current to increase [22]. Since the C-profile overlaps the P implant, the C-related defects are in the collector region, primarily near the collector/substrate junction, see Fig. 4. It may influence the collector sheet resistivity and the leakage currents of the collector/base and even more the collector/substrate junction. The sheet resistivity of the standard collector is  $\sim 356 \Omega/\square$ , whereas higher values of 544 and  $630 \Omega/\square$  are measured for the 2 and  $5 \times 10^{14} / \text{cm}^2$  C implanted structures, respectively. The C-related defects probably lower the mobility of the carriers, hereby increasing the resistivity of the collector. No change in sheet resistivity of the base was observed.

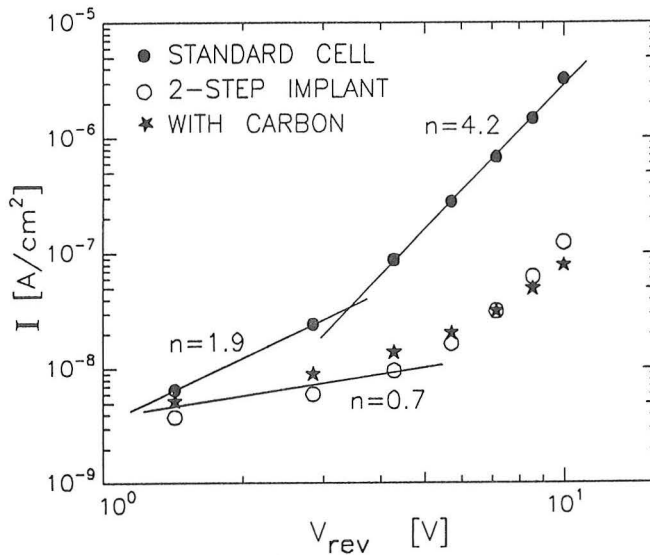


Fig. 9. Reverse I-V characteristics of the collector/base junction.  $I \propto V^n$ , where  $n \approx 0.5$  for an ideal junction and  $2 < n < 4$  for a junction containing dislocations.

The C-related defects also introduce states in the bandgap which enhance carrier generation/recombination. The position of these states can be determined by temperature dependent leakage current measurements [22], shown in Fig. 10 for C implanted diodes. The leakage in the C-implanted collector/base junctions increases with temperature and can be fitted with an activation energy between 0.55 and 0.60 eV for both C doses. This activation energy indicates that deep traps in the depletion region are generated by the implants. Such deep traps have been observed for MeV C implanted silicon [22], although activation energies of  $\sim 0.6$  eV also have been found for junctions containing dislocations [19]. The lowest leakage is observed for the highest C dose, which is attributed to the stronger gettering of point defects and impurities from the depletion region. The leakage current density at 25°C is only  $\sim 10$  nA/cm<sup>2</sup>, which is a good result.

Figure 11 shows the temperature dependent leakage current density of the collector/substrate junction for C implanted diodes. The current density here is on the order of 100 mA/cm<sup>2</sup>, 7 orders of magnitude higher than for the collector/base junction. This is attributed to the high concentration of C-related defects positioned near the collector/substrate junction. A small decrease in leakage current density for increasing measuring temperature is observed, see also Wang *et al.* [23].

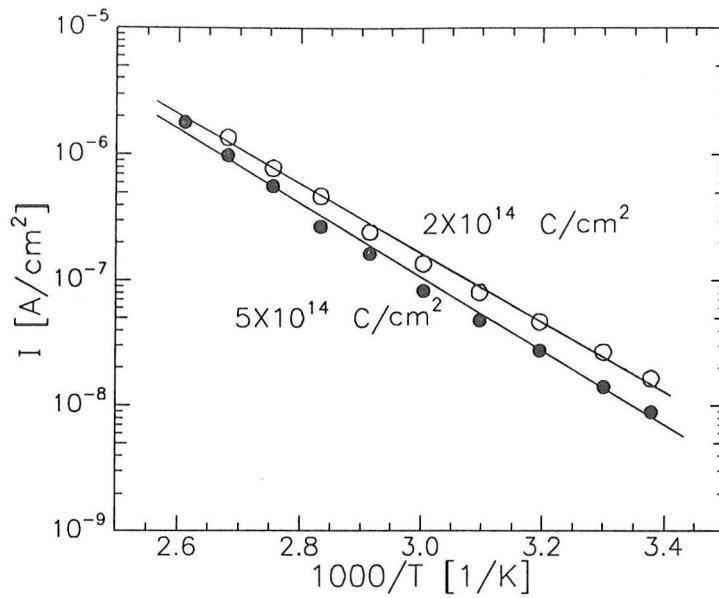


Fig. 10. Leakage current density as a function of  $1/T$  for collector/base junctions implanted with 1.15 MeV C, measured at reverse bias of 2.85 V. Activation energies between 0.55 and 0.60 eV are extracted (drawn lines).

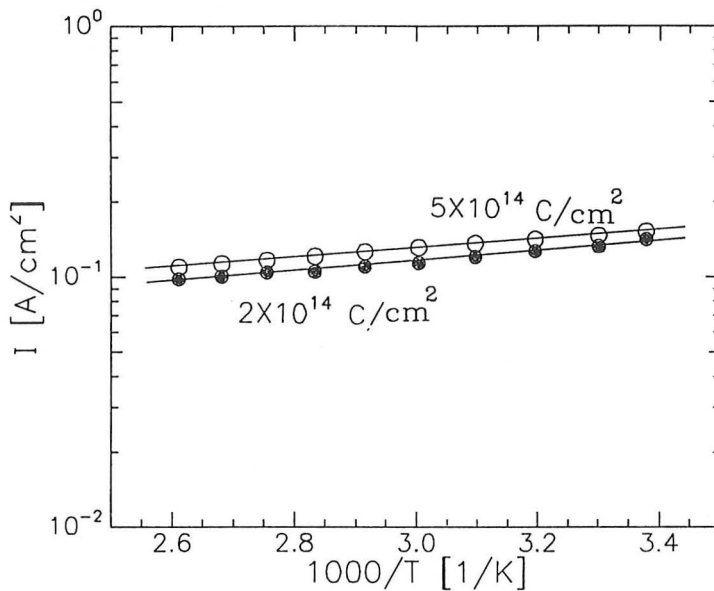


Fig. 11. Leakage current density as a function of  $1/T$  for collector/substrate junctions implanted with 1.15 MeV C, measured at reverse bias of 2.85 V. Leakage decreases with increasing temperature.

#### 4. DISCUSSION AND CONCLUSIONS

High-energy ion implantation was used for creating the collector in vertical bipolar transistors, but dislocations formed during annealing and severely influenced device performance. The collector/base junction showed an increase in leakage current when the junction was intersected by dislocations. If the base/emitter and collector/base junctions were intersected, c-e shorts arose probably as a result of enhanced diffusion of the emitter dopant along a dislocation. These shorts reduced the yield of transistors with a  $10^4 \mu\text{m}^2$  emitter area to less than 35%.

Two methods were applied in this chapter to suppress dislocation formation for the collector implant. In the first scheme, the collector was formed in two implant and anneal steps, and in the second scheme, extra carbon to doses of 2 and  $5 \times 10^{14} / \text{cm}^2$  was implanted in the collector region prior to annealing. For both methods, dislocation formation was avoided and the leakage current in the collector/base junction decreased. Also, for the transistors with 2-step implanted collectors, only 1 out of 30 transistors showed an excessive collector current at low base-emitter voltage. For the C co-implanted collectors, none of the transistors were shorted. However, for the C implanted junctions, C-related defects introduced deep traps in the bandgap which gave rise to an increase in leakage current especially at the collector/substrate junction, because the concentration of defects is highest near this junction.

The optimum collector dose is  $\sim 4 \times 10^{13} \text{ P/cm}^2$  [3]. For the multi step method, only 2-steps are needed in total for implanting this dose. This means that only one additional series of masking/implant/anneal steps has to be performed. The extra masking step is necessary since the LOCOS oxide is not thick enough to stop the P ions. If doses much higher than  $4 \times 10^{13} \text{ P/cm}^2$  are required, the multi step procedure would involve too many extra implant and anneal steps.

Dislocation formation for P doses as high as  $1 \times 10^{15} / \text{cm}^2$  can be avoided by co-implanting C [15]. In this case, only one extra implant step has to be carried out. The C layer is known to efficiently getter point defects and metallic impurities from the near surface region, thereby improving the quality of the active regions of the device [17,22,23]. However, the C-related defects should not influence the leakage of either of the junctions too much. This may be reached by lowering the C dose to the minimum value needed for suppressing dislocation formation for the P implant. Also, the C can be implanted at a somewhat lower energy such that it is positioned in between the collector/base and the collector/substrate junctions, or at a much

higher energy so that it is below the collector/substrate junction. However, it should be investigated if dislocation formation is then still avoided.

## ACKNOWLEDGEMENTS

The authors wish to thank Gerrit Boom for processing the devices and Karel Lippe for helping with the electrical characterization.

## REFERENCES

- [1] R.D. Rung, C.J. Dell'Oca, and L.G. Walker, *IEEE Trans. Electron Devices* ED-28, 1115 (1981).
- [2] J.Y. Chen, *IEEE Trans. Electron Devices* ED-31, 910 (1984).
- [3] R.C.M. Wijburg, G.J. Hemink, J. Middelhoek, and H. Wallinga, *Proc. ESSDERC*, 515 (1990).
- [4] F.S. Lai, L.K. Wang, Y. Taur, J.Y. Sun, K.E. Petrillo, S.K. Chicotka, E.J. Petrillo, M.R. Polcari, T.J. Bucelot, and D.S. Zicherman, *IEEE Trans. Electron Devices* ED-33, 1308 (1986).
- [5] J.F. Ziegler, B.L. Crowder, and W.J. Kleinfelder, *IBM J. Res. Dev.* 15, 452 (1971).
- [6] H.J. Böhm, L. Bernewitz, W.R. Böhm, and R. Köpl, *IEEE Trans. Electron Devices* ED-35, 1616 (1988).
- [7] A. Mouthaan, and M. Vertregt, *Solid State Electronics* 29, 1289 (1986).
- [8] R.C.M. Wijburg, G.J. Hemink, J. Middelhoek, H. Wallinga, and A. Mouthaan, *IEEE Trans. Electron Devices* ED-38, 11 (1991).
- [9] M. Takahashi, S. Konaka, and A. Kajiyama, *J. Appl. Phys.* 54, 6041 (1983).
- [10] M. Tamura, *Mater. Sci. Rept.* 6, 141 (1991).
- [11] R.J. Schreutelkamp, J.S. Custer, J.R. Liefing, W.X. Lu and F.W. Saris, *Mater. Sci. Rept.* 6, 275 (1991).
- [12] F.W. Ragay, "High-energy ion implantation for bipolar transistor fabrication," PhD-thesis, University of Twente, The Netherlands, 1991.
- [13] J.R. Liefing, V. Raineri, J.S. Custer, R.J. Schreutelkamp, and F.W. Saris, *Mat. Res. Soc. Symp. Proc.* 235 *in press*.
- [14] R.J. Schreutelkamp, J.R. Liefing, J.S. Custer, and F.W. Saris, *Appl. Phys. Lett.* 58, 2827 (1991).

- [15] M. Tamura, T. Ando, and K. Ohyu, Nucl. Instr. and Meth. **B59/60**, 572 (1991).
- [16] J.R. Liefting, J.S. Custer, and F.W. Saris, Mat. Res. Soc. Symp. Proc. **235**, *in press*.
- [17] H. Wong, J. Lou, N.W. Cheung, E.P. Kvam, K.M. Yu, D.A. Olson, and J. Washburn, Appl. Phys. Lett. **57**, 798 (1989).
- [18] S.M. Sze, "*Semiconductor Devices: Physics and technology*," John Wiley & Sons, New York, 1985.
- [19] P. Ashburn, C. Bull, K.H. Nicholas, and G.R. Booker, Sol. St. Elec. **20**. 731 (1977).
- [20] K.V. Ravi, "*Imperfections and Impurities in Semiconductor Silicon* " John Wiley & Sons, New York, 1981.
- [21] C. Bull, P. Ashburn, G.R. Booker, and K.H. Nicholas, Solid State Electronics **22**. 95 (1979).
- [22] H. Wong and N.W. Cheung, Nucl. Instr. and Meth. **B37/38**, 970 (1989).
- [23] A.C.M. Wang and S. Kakihana, IEEE Trans. Electron Devices, ED-21, 667 (1974).
- [24] W. Skorupa, R. Kögler, K. Schmalz, and H. Bartsch, Nucl. Instr. and Meth. **B55**, 224 (1991).
- [25] K. Tsukamoto, S. Komori, T. Kuroi, and Y. Akasaka, Nucl. Instr. and Meth. **B59/60**, 584 (1991).





## CHAPTER 6

---

### GETTERING OF Cu AT BURIED DAMAGE LAYERS MADE BY Si SELF IMPLANTATION

*Buried amorphous Si (a-Si) layers were obtained by 100 keV  $^{28}\text{Si}$  channeled implants into p-type Si(100). Before and after recrystallization of the a-Si layer, Cu was implanted at keV energies for doses ranging from  $5 \times 10^{13}$  to  $1 \times 10^{15}$   $\text{cm}^{-2}$  to obtain a high concentration of Cu in the near surface region. For comparison, Cu was also implanted into crystalline Si. After the Cu implants, anneals were performed at temperatures between 490 and 900 °C for times ranging from 10 to 320 min. Cu profiles before and after annealing were studied with Rutherford backscattering spectrometry and channeling analysis. In case Cu was implanted after recrystallization of the buried amorphous layer, Cu gettered at the position where the amorphous/crystalline interfaces met during recrystallization. If Cu was implanted before recrystallization, Cu diffused towards the buried a-Si region upon annealing and was trapped inside the recrystallizing buried amorphous layer. The results show that buried damage layers can effectively getter Cu from the Si surface layer and gettering is most efficient at 600 °C.*

## 1. INTRODUCTION

Gettering is a useful technique for removing metallic impurities from the active regions of a device. These metallic impurities, like Cu, Fe, and Au, can act as generation recombination (GR) centres within the bandgap. These GR centres increase the leakage current and reduce the minority carrier lifetime, thereby degrading the quality of devices [1].

One way to induce gettering is by ion-implantation at the front or back surface of a wafer. Species like C, N, O, Ne, and Ar have already been used for this purpose [2]. It has been found that at least four different trapping regions can be identified: (a) the surface, (b) the region of primary defects, (c) the doped layer, and (d) the region of recoiled host atoms [3]. It is not always clear whether gettering is induced by the implanted ion or by the damage sites created during implantation [2].

We have studied gettering of Cu at buried damage layers made by Si self implantation. In this way, gettering can only be attributed to trapping of Cu at damage created by the Si implant. We have investigated gettering before and after recrystallization of the buried amorphous layer. The stability of Cu trapping as a function of temperature has also been investigated.

## 2. EXPERIMENTAL

Implants of 100 keV Si were done in *p*-type (100) silicon along [100] direction at room temperature with an ASM 220 medium current ion implanter [4]. Beam contamination due to  $N_2^+$  was determined to be less than 1%, by measuring the ratios of the silicon isotopes present in the beam before implantation and comparing with the natural abundances. Implants of 15 to 19 keV Cu to doses of  $4.3 \times 10^{13}$  to  $2.4 \times 10^{15} / \text{cm}^2$  were done with the MeV ion implant facility at the FOM-institute [5]. The current density during implantation was kept below  $50 \text{ nA/cm}^2$ , thereby minimizing beam heating effects. Annealing treatments were performed in a vacuum furnace at a base pressure of  $10^{-7}$  Torr. Copper profiles were measured by means of Rutherford backscattering spectrometry (RBS) in channeling analysis with a 2 MeV  $\text{He}^+$  beam. For Cu implants into crystalline silicon (c-Si), the profiles were measured at a backscattering angle of  $\theta = 95^\circ$ , whereas all the other profiles were measured at an angle of  $\theta = 120^\circ$ .

### 3. RESULTS AND DISCUSSION

Copper was implanted into c-Si to study damage formation and Cu diffusion in the absence of a buried amorphous layer. In Fig. 1a and b, RBS channeling spectra of Cu implanted at an energy of 19 keV and doses of  $4.3 \times 10^{13}$ ,  $8.7 \times 10^{13}$ ,  $4.3 \times 10^{14}$ , and  $8.7 \times 10^{14} / \text{cm}^2$  into c-Si are shown. Notice that in these two spectra,

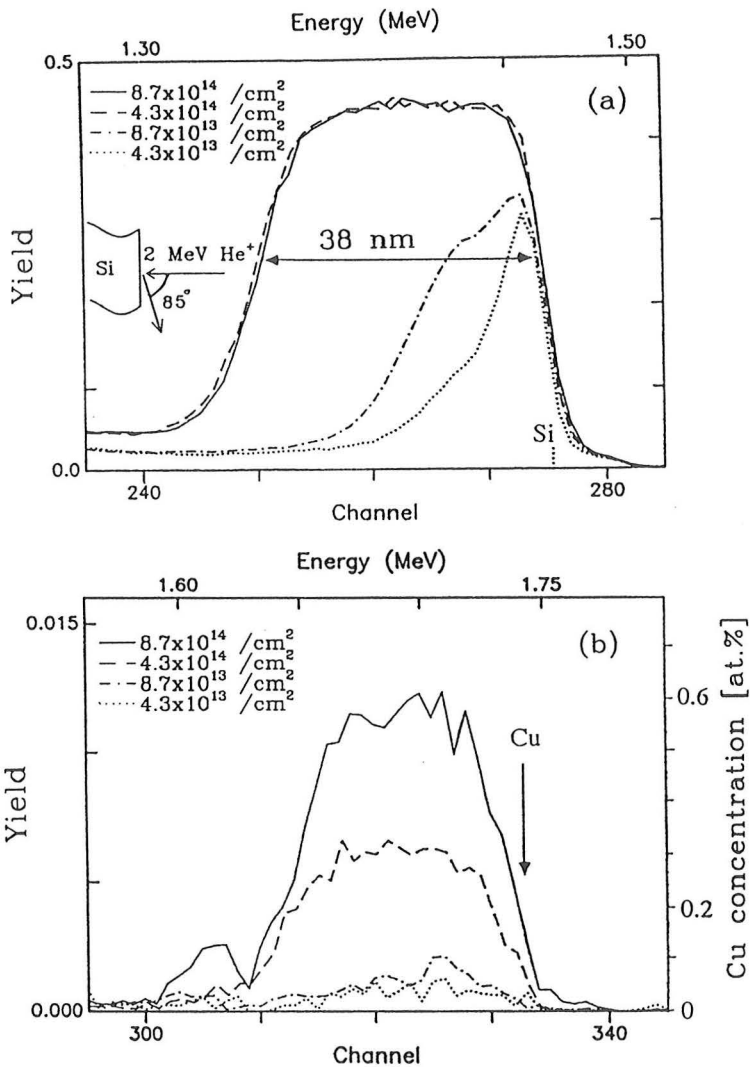


Fig. 1. RBS channeling spectra of Si implanted with 19 keV Cu for four different doses. (a) damage in the Si. (b) Cu profiles.

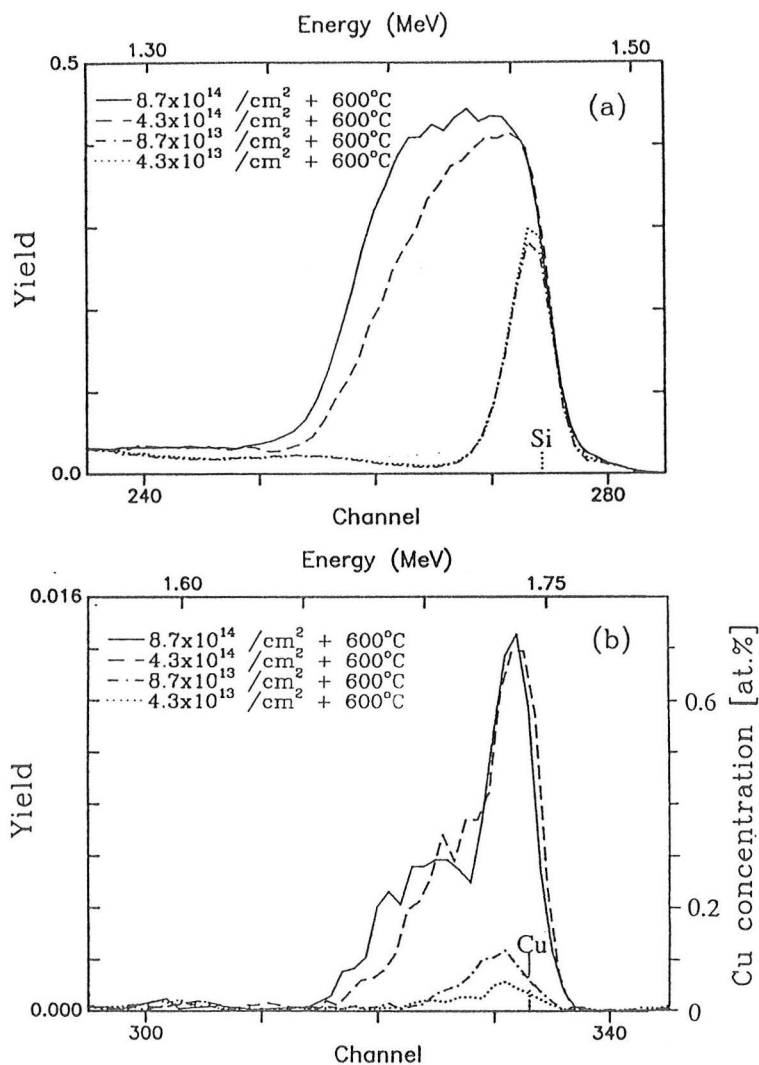


Fig. 2. RBS channeling measurements of Si implanted with 19 keV Cu after 600°C, 1 hr annealing. (a) damage in the Si. (b) Cu profiles.

and also in the following RBS spectra, the number of channels along the horizontal axis is the same for Fig. a and b. This means that the depth range is nearly equal for Fig. a and b.

The damage in the Si created by the Cu implant is shown in Fig. 1a. For  $4.3$  and  $8.7 \times 10^{14} \text{ Cu/cm}^2$  implants, an amorphous surface layer with a thickness of  $\sim 38 \text{ nm}$  formed. For lower doses, a highly defective crystalline region resulted. The Cu part of the spectrum is shown in Fig. 1b. The atomic concentration of the Cu is given

on the right vertical axis. The Cu profile peaks at a depth of 19 nm and has a full width half maximum of 26 nm. By comparing the Cu profile width and the damage width, it is clear that the Cu is in the damaged regions. Hence, for  $4.3$  and  $8.7 \times 10^{14}$  Cu/cm<sup>2</sup>, most of the Cu is inside the amorphous layer. For  $4.3$  and  $8.7 \times 10^{13}$  Cu/cm<sup>2</sup> no amorphous layer was formed, so the Cu for these implants is in a highly defective region.

The channeling spectra after 600°C, 1 hr annealing are shown in Fig. 2a and b. For the highest Cu doses, there is still a highly defective layer at the surface after the anneal (Fig. 2a). For the low doses, the amount of dechanneling has decreased strongly. In Fig. 2b, the Cu part of the channeling spectrum is shown. Measurements in random and channeling direction gave the same Cu profiles, indicating that no Cu was on substitutional sites. The Cu has moved towards the surface for all four doses. For the two higher doses, the Cu remained inside the amorphous layer during regrowth, as earlier observed by Custer *et al.* [6]. The concentration of Cu at the surface was at least 0.7 at.% for both doses, but this is an underestimate since detector resolution prevents the exact determination of the maximum concentration. Also for the two low doses, where no amorphous layer formed, Cu diffused towards the surface during the 600°C, 1 hr anneal. So in this case, the Cu was trapped at the damage sites created during implantation.

For the highest dose,  $8.7 \times 10^{14}$  /cm<sup>2</sup>, almost half the Cu diffused into the crystal during annealing and could not be detected by RBS. For the three other Cu doses, no Cu was lost during annealing. If the samples are annealed at 900°C for 1 hr (spectra not shown) the damage in the Si greatly reduced and all the Cu diffused into the bulk.

For investigation of Cu gettering at buried damage layers, 100 keV  $1 \times 10^{15}$  /cm<sup>2</sup> channeling Si implants into Si (100) were done. In this way, buried amorphous layers with a thickness of 140 nm were created underneath a crystalline surface layer of 60 nm. After the Si implants,  $1.1 \times 10^{15}$  /cm<sup>2</sup> 15 keV Cu implants were done.

In Fig. 3a, the damage in the silicon after the double implant is shown as a solid line. The scattering peak around channel 235 is due to the damage caused by the Cu implant. Gettering at the buried amorphous layer was studied as a function of anneal time at a temperature of 490°C. After 10 min, the buried layer partially recrystallized and the damage created by the Cu implant partially annealed. The Cu diffused to the recrystallizing buried amorphous layer (Fig. 3b). The atomic concentration of Cu in the a-Si layer after an anneal of 10 min was 0.07 at.%. For longer anneals, the Cu was confined in the regrowing buried amorphous layer. After 320 min, the layer recrystallized and most of the Cu is found at the defect

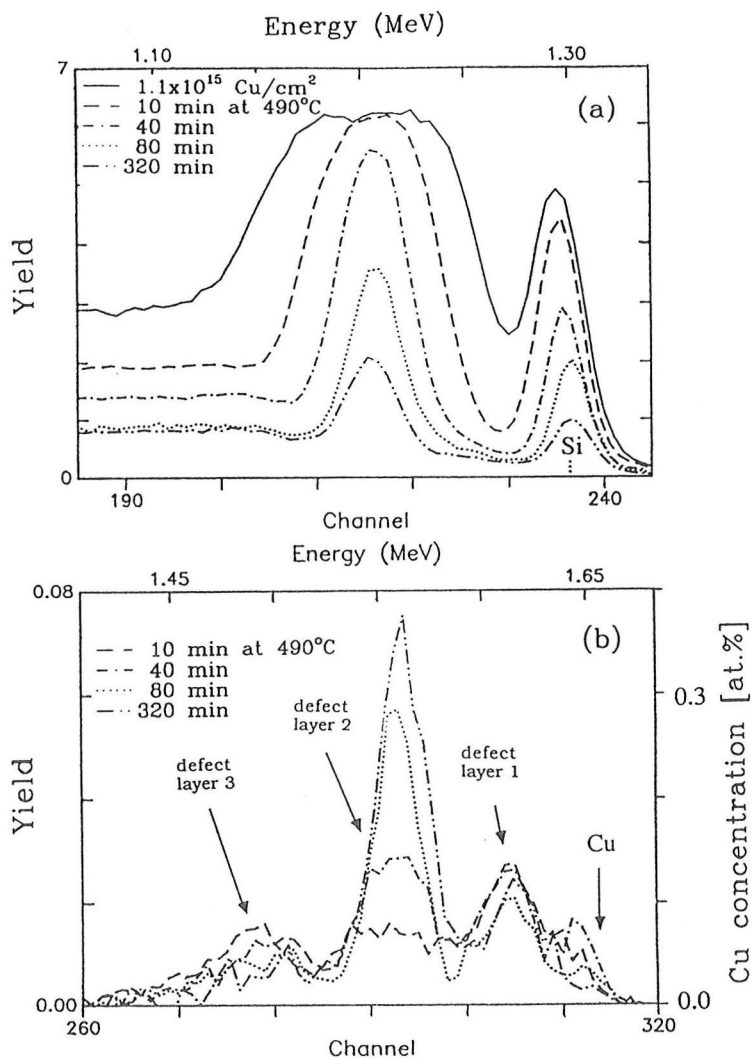


Fig. 3. RBS channeling spectra of Si with a 140 nm buried amorphous layer and implanted with  $1.1 \times 10^{15} / \text{cm}^2$  15 keV Cu. Anneals were performed at 490°C for 10 to 320 min. (a) damage in the Si. (b) Cu profiles.

layer where the two moving a/c- interfaces met during recrystallization. This layer is identified as defect layer 2 in Fig. 3b. The atomic concentration of the Cu at this defect layer was at least 0.4 at.%. Defect layers 1 and 3 are at the position of the original a/c-transition regions at the surface- and substrate side, respectively, and are the result of incomplete recrystallization [7]. Gettering of Cu is stronger at

defect layer 1 than at defect layer 3. During annealing at 490°C, the Cu concentrations in defect layers 1 and 3 decreased while the concentration in layer 2 increased.

Gettering was also studied as a function of anneal temperature. In Fig. 4, RBS spectra are shown for samples implanted with  $1.1 \times 10^{15}$  Cu/cm<sup>2</sup> before crystallization of the buried amorphous layer. After implantation, the samples were annealed at temperatures between 490 and 900°C. In Fig. 4a, the dechanneling in the Si is shown for the different temperatures. The scattering peak near the Si surface channel, caused by the Cu implant, decreases if the anneal temperature increases, indicating that more damage anneals at higher temperatures. The scattering peak near channel 220, which is due to dechanneling at the second defect layer, is highest for 600°C and lowest for 900°C annealing.

The Cu profiles after these anneals are shown in Fig. 4b. Gettering of Cu at the first defect layer was highest for 490°C and lowest for annealing at 900°C. For 600°C annealing,  $7 \times 10^{14}$  Cu/cm<sup>2</sup> gettered at the second defect layer, giving rise to an atomic concentration of at least 0.6 at.%. This was the highest for all temperatures, but still an underestimate because of the limited detector resolution. At 900°C, no trapping could be seen anymore by RBS. No gettering of Cu was seen at the third defect layer for all anneal temperatures.

Copper gettering was also investigated for Cu implants performed *after* crystallization of the buried amorphous layer. In Fig. 5, RBS spectra are shown for 15 keV Cu implants to doses of 4.2 and  $8 \times 10^{14}$  /cm<sup>2</sup> in samples where the buried amorphous layer has already been regrown. In Fig. 5a, the dechanneling in the Si caused by the Cu implants is presented. After annealing at 600°C for 1 hr, the dechanneling greatly reduced at the position where Cu was implanted.

The Cu profiles of the as-implanted samples are shown in Fig. 5b. During annealing, some of the Cu gettered at the buried defect layers 1 and 2 and some diffused into the bulk. For the  $4.2 \times 10^{14}$  /cm<sup>2</sup> implant,  $1.6$  and  $1.5 \times 10^{14}$  Cu/cm<sup>2</sup> gettered at the first and second defect layer, respectively. For the  $8 \times 10^{14}$  /cm<sup>2</sup> implant,  $1.3 \times 10^{14}$  Cu/cm<sup>2</sup> gettered at defect layer 1 and  $2.7 \times 10^{14}$  Cu/cm<sup>2</sup> at defect layer 2. No gettering at the third defect layer is observed by RBS. The remaining Cu is assumed to have diffused into the bulk of the silicon.

Gettering of Cu was also studied for buried amorphous Si layers positioned at large depth. An example of this is shown in Fig. 6. A buried amorphous layer at a depth of 1.6 μm and a thickness of 0.7 μm was created by a 1.7 MeV Si implant. Then, a 490°C, 15 min anneal was performed to remove damage in the crystalline surface layer. In this sample, Cu was implanted at 15 keV to a dose of

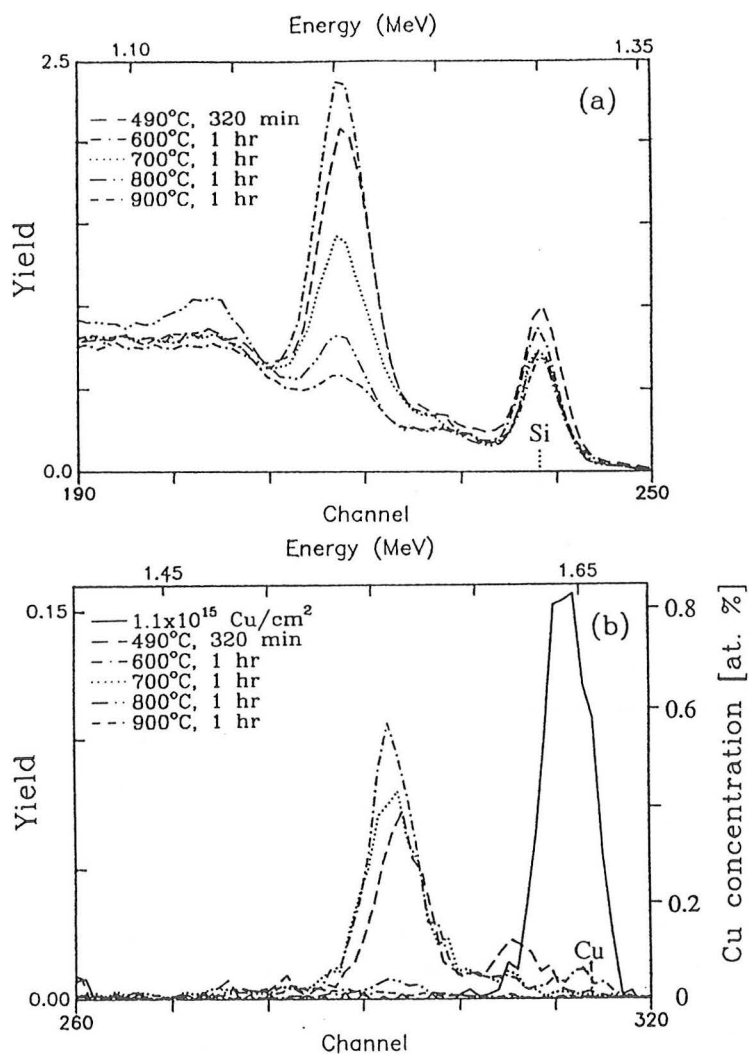


Fig. 4. RBS channeling spectra of Si with a 140 nm buried amorphous layer implanted with  $1.1 \times 10^{15} / \text{cm}^2$  15 keV Cu. Anneals were done at 490 to 900°C. (a) damage in the Si. (b) Cu profiles.

$2.4 \times 10^{15} / \text{cm}^2$ . The Si part of the RBS spectrum of this sample is shown in Fig. 6a. The scattering peak at channel 200 is due to the damage created by the Cu implant. After Cu implantation, an anneal was performed at 600°C for 1 hr to fully recrystallize the buried amorphous layer. In Fig. 6a, spectra are shown after such an anneal for samples with and without the Cu implant. For the sample without Cu,

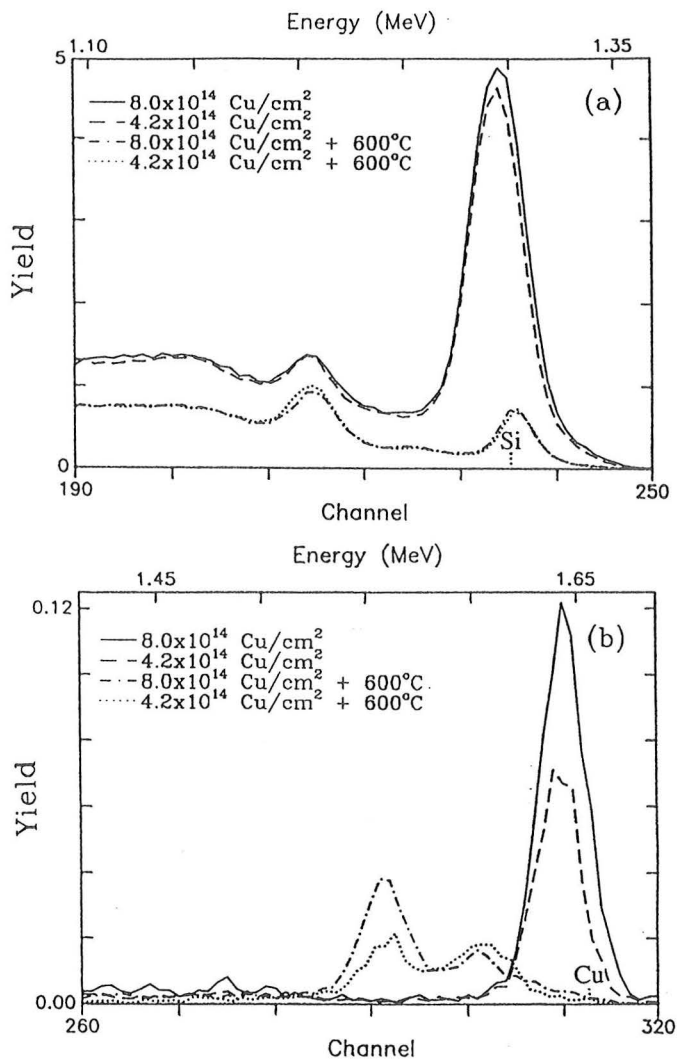


Fig. 5. RBS channeling spectra of Cu implants after crystallization of the buried amorphous layer. Final annealing was done at 600°C for 1 hr. (a) damage in the Si. (b) Cu profiles.

only a small amount of dechanneling can be observed around channel 80. This is the position where the two moving *a/c*-interfaces met during recrystallization. For the sample with Cu, more dechanneling is observed near channel 80, showing that the Cu inhibits the annealing of damage.

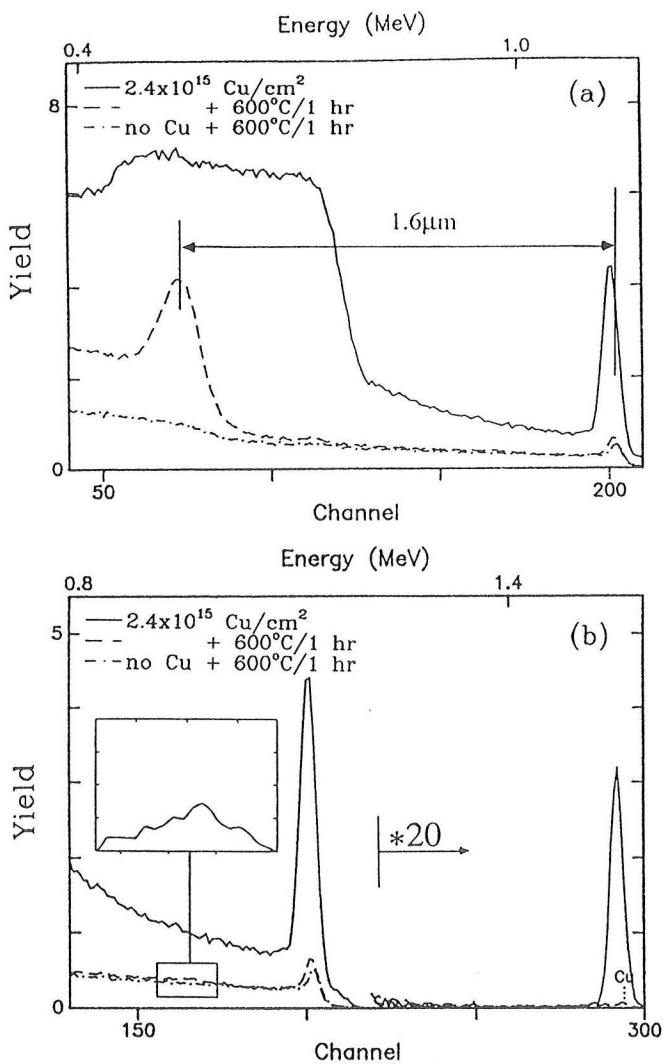


Fig. 6. RBS channeling spectra of Si with a 1.6 μm buried amorphous layer. Final annealing was carried out at 600°C for 1 hr. (a) damage in the Si. (b) Cu profiles.

The Cu part of the spectrum as well as the Si surface part before and after the 600°C anneal are shown in Fig. 6b. After annealing, there is only a small amount of Cu left at the surface regions. The Cu which gettered at the buried defect layer gives rise to a small direct scattering peak around channel 170. In the insert, a

magnification of the scattering peak is shown. The amount of gettered Cu is estimated to be on the order of  $1 \times 10^{15} / \text{cm}^2$ .

#### 4. CONCLUSIONS

Our results show that buried damage layers can effectively getter Cu from the Si surface layer and that gettering is most efficient for anneals performed at 600°C. If the buried damage layers are produced by MeV implants, they may be used to getter Cu from the active device regions at a depth of several microns.

#### ACKNOWLEDGEMENTS

We would like to thank R.E. Kaim from the Varian/Extrion division in Beverly for performing the channeled Si implants.

#### REFERENCES

- [1] J.R. Monkowski, *Solid State Technol.* **24**, 44 (1981).
- [2] H. Wong and N.W. Cheung, *Appl. Phys. Lett.* **52**, 889 (1988).
- [3] D. Lecrosnier, *Nucl. Instr. and Meth.* **209/210**, 325 (1983).
- [4] D.W. Berrian, R.E. Kaim, J.W. Vanderpot, and J.F.M. Westendorp, *Nucl. Instr. and Meth.* **B37/38**, 500 (1989).
- [5] A. Polman *et al.*, *Nucl. Instr. and Meth.* **B37/38**, 935 (1989).
- [6] J.S. Custer, Micheal O. Thompson, and J.M. Poate, *Mater. Res. Soc. Symp. Proc.* **128**, 545 (1988).
- [7] K.S. Jones, S. Prussin, and E.R. Weber, *Appl. Phys. A* **45**, 1 (1988).



## SUMMARY

Ion implantation is used in the semiconductor industry with great success for introducing dopants into silicon. However, damage is generated by the implanted ions, giving rise to secondary defect formation during thermal treatment. These secondary defects can have detrimental influence on device performance and are a major topic in research today. This thesis studies how secondary defect formation can be influenced by altering implant or anneal conditions, and how this affects device performance.

Chapter 1 introduces the criterion for the formation of dislocations (pre-amorphization damage) by discussing dislocation formation for 1 MeV In implants. There, it is shown that the initial defect evolution during 900°C annealing of amounts of primary damage just below and above the critical amount is in principle the same. However, for prolonged annealing, only the secondary defects formed for the highest amount of damage grow large enough to form stable dislocations.

Chapter 2 investigates first dislocation formation for low and high mass implants. It is shown that the critical number of displaced Si atoms, needed for the formation of dislocations for B implants, is the *total* number of Si atoms displaced by the incoming B ions. The structure of defect complexes formed during implantation, which is altered by changing *e.g.* the implant temperature or the current density, is not so critical. For 1 MeV In implants, where the implant damage consists mainly of amorphous zones, an increase in critical dose for dislocation formation of  $\sim 3$  is observed if the implant temperature is raised. This is attributed to the interaction of point defects with the amorphous zones during the high temperature implant. Secondly, it is shown that annealing RT implants of 150 keV In results in end-of-range dislocation loop formation, whereas performing the implant at 300°C suppresses amorphization and pre-amorphization damage forms again. Thirdly, it is demonstrated that amorphizing Ge implants done at liquid nitrogen instead of room temperature reduces the number of Si interstitials in the amorphous/crystalline transition region below the critical number needed for dislocation formation. Therefore, dislocations are not observed after high temperature annealing of the liquid nitrogen temperature implants.

In Chapter 3, an example of defect engineering is presented. Single step implants of B, P, and As result in dislocation formation if a critical amount of damage is created during the implant. However, higher doses could be implanted if a sequence of implant and anneal steps is applied, where each implant step generates

a sub-critical amount of damage. This is shown for keV implants of B and MeV implants of B, P, and As.

Chapter 4 shows that annealing carbon implant damage does not result in dislocation formation even for doses > 100 times higher than that required for B implants. Hence, C is an exception in the criterion for dislocation formation. Carbon is believed to interact with the displaced Si atoms, thereby preventing the interstitials to agglomerate and form dislocations. C is also able to avoid dislocation formation of co-implanted B ions. The C dose needed to avoid dislocation formation for the B implant increases nonlinearly with B dose. Special C-related secondary defects remain after annealing if the C dose is higher than  $4 \times 10^{15} / \text{cm}^2$ .

Chapter 5 presents results of electrical measurements on vertical bipolar transistors formed by high-energy ion implantation. Secondary defects, resulting from annealing of implant damage, give rise to an increased leakage current and to collector-emitter shorts. These shorts reduce the yield of good transistors with large emitter areas to only 30%. The two ways of defect engineering, as discussed in chapter 3 and 4, were introduced in the fabrication process to avoid dislocation formation for the high-energy collector implant. For both methods, dislocation formation was avoided and the leakage in the collector/base junction consequently decreased. Also, for the 2-step implanted collectors, only 1 out of 30 transistors showed an excessive collector current at low base-emitter voltage. For the C co-implanted collectors, the transistor yield increased to even 100%.

Until now, dislocations are considered to have a negative influence on the quality of silicon devices. This is true if the dislocations are in the depletion region of a junction and trap metallic impurities. However, this damage can also be generated at large depth, far beyond the active regions of the device, where it can act as a gettering layer for metallic impurities like Cu. Chapter 6 shows that this trapping occurs very efficiently for buried damage layers and that gettering is most efficient at 600°C. If the buried damage layers are produced by MeV implantation, they may be used to getter Cu from the active device area at a depth of several microns.

## SAMENVATTING

Ionen implantatie wordt met veel succes in de halfgeleiderindustrie gebruikt om silicium te doteren. De geïmplanteerde ionen veroorzaken echter schade, wat aanleiding geeft tot de vorming van secundaire defecten tijdens een warmtebehandeling. Deze secundaire defecten kunnen een desastreuze invloed hebben op het gedrag van elektronische schakelingen en zijn daarom een belangrijk onderwerp in het hedendaagse onderzoek. Dit proefschrift beschrijft hoe de vorming van secundaire defecten beïnvloed kan worden door een verandering van implantatie- of verwarmingscondities, en hoe dit het gedrag van elektronische schakelingen beïnvloedt.

Hoofdstuk 1 introduceert het criterium voor dislocatievorming (pre-amorfisatie schade) met als voorbeeld 1 MeV indium implantaties. Daar wordt aangetoond dat de eerste defect evolutie tijdens een warmtebehandeling bij 900°C, van hoeveelheden schade net onder en boven de kritische hoeveelheid, in principe hetzelfde is. Maar als de warmtebehandeling voortgezet wordt, blijkt dat alleen voor de grootste hoeveelheid schade de secundaire defecten groot genoeg worden om stabiele dislocaties te kunnen vormen.

Hoofdstuk 2 beschrijft ten eerste een verschil in dislocatievorming na implantatie van ionen met lage of hoge massa. Voor dislocatie vorming bij B ionen implantatie is alleen het *totaal* aantal verplaatste Si atomen van belang. Dit *totaal* aantal wordt niet beïnvloed door een verandering in implantatietemperatuur of stroomdichtheid. Voor 1 MeV In implantaties, waar de implantatieschade hoofdzakelijk uit amorfe zones bestaat, neemt de kritische dosis voor dislocatie vorming toe als de implantatie temperatuur toeneemt. Dit wordt toegeschreven aan de interactie van puntdefecten met de rekristalliserende amorfe zones tijdens de hete implantatie. Als de implantatietemperatuur boven 300°C stijgt, neemt de kritische hoeveelheid verplaatste Si atomen af tot  $\sim 10^{16}$  /cm<sup>2</sup>, ongeveer het aantal voor B implantaties waarvoor geen amorfe zones worden gevormd. Ten tweede wordt gedemonstreerd dat 150 keV In implantaties uitgevoerd bij 300°C amorfisatie onderdrukt. Na verwarming tot 900°C ontstaat pre-amorfisatie schade in plaats van *end-of-range* (EOR) dislocaties. Ten derde wordt aangetoond dat EOR-dislocaties niet ontstaan voor amorfiserende 75 keV Ge implantaties uitgevoerd bij vloeibare stikstof temperatuur, omdat het aantal verplaatste Si atomen in het amorf/kristallijne overgangsgebied kleiner is dan het kritische getal nodig voor dislocatievorming.

In hoofdstuk 3 wordt een voorbeeld van "defect engineering" gepresenteerd. Eénstaps implantaties van B, P en As resulteren in dislocaties na een

warmtebehandeling. Hogere doses kunnen echter geïmplanteerd worden als een serie van implantatie- en verwarmingsstappen wordt toegepast, waarbij elke implantatiestap een sub-kritische hoeveelheid schade veroorzaakt.

Hoofdstuk 4 laat zien dat C een uitzondering op het criterium voor dislocatievorming is omdat dislocaties niet ontstaan voor C implantaties, zelfs niet voor doses 100 keer groter dan nodig voor B implantaties. Het idee is dat C een interactie aangaat met de verplaatste Si atomen en op die manier vermijdt dat de interstitiële samenklonteren en dislocaties vormen. C blijkt ook in staat de vorming van dislocaties tegen te gaan van mede geïmplanteerde B ionen. De C dosis, welke nodig is om dislocaties bij de B implantatie tegen te gaan, neemt niet-lineair toe met de B dosis. Speciale C gerelateerde secundaire defecten blijven achter na de warmtebehandeling als de C dosis hoger is dan  $4 \times 10^{15} / \text{cm}^2$ .

Hoofdstuk 5 presenteert resultaten van elektrische metingen aan verticale bipolaire transistoren gemaakt m.b.v. hoge-energie ionen implantatie. Secundaire defecten, resulterend na de warmtebehandeling van de implantatieschade, geven aanleiding tot een verhoogde lekstroom en tot collector-emitter kortsluitingen. Deze kortsluitingen verminderen de opbrengst aan werkende transistoren met grote emitter oppervlaktes tot slechts 30%. De twee methoden van "defect engineering" uit hoofdstuk 3 en 4 zijn geïntroduceerd in het productieproces. Beide methoden blijken in staat om dislocaties te vermijden en de lek in de collector/basis-overgang vermindert dienovereenkomstig. Voor de collectoren welke in 2 stappen waren geïmplanteerd, vertoonde maar 1 van de 30 transistoren een sterk verhoogde collectorstroom bij lage basis-emitter spanning. Voor de collectoren die met extra C geïmplanteerd waren, was de transistoropbrengst zelfs 100%.

Tot nu toe is gesteld dat dislocaties alleen maar een negatieve invloed op de kwaliteit van elektronische schakelingen kunnen hebben. Dit is waar als zij in een actief gebied zitten van een elektronische schakeling en daar metaal verontreinigingen invangen. Maar schade kan ook op een grotere diepte opgewekt worden, waar het als een absorptielaag voor metaalverontreinigingen zoals Cu kan fungeren. Hoofdstuk 6 laat zien dat het invangen van metaalverontreinigingen voor begraven schade optimaal is bij een verwarmingstemperatuur van  $600^\circ\text{C}$ . Als de begraven schade gemaakt wordt op een diepte van enkele micrometers m.b.v. MeV implantaties, kan deze gebruikt worden om Cu uit de actieve gebieden van elektronische schakelingen in te vangen.

## NAWOORD

In de vier jaar die ik nodig had voor mijn promotie hebben velen mij met raad en daad bijgestaan. Sommigen van hen wil ik hier graag expliciet vermelden.

Ten eerste wil ik mijn promotoren en assistent-promotor bedanken. Frans Saris had de stimulerende eigenschap nooit de duisternis te zien, maar altijd alleen maar dat ene lichtpuntje. Dit zorgde ervoor dat het onderzoek nooit te lang bleef hangen in gebieden waar toch niet uit te komen was. Ik ben Hans Wallinga dankbaar dat hij mij de vrijheid heeft geboden om zelf een invulling te geven aan het promotie onderzoek. Daarnaast ben ik Jon Custer zeer erkentelijk, die niet alleen de strengste referee was die ik heb mogen meemaken, maar daarnaast ook nog een uitstekende receptionist, postbezorger en typist was.

Simon Doorn, Johan Derks, Jan ter Beek, en Richard Loos zijn een onmisbare steun geweest bij het oplossen van vele technische problemen. Henk Sodenkamp en Jan Vanhellemont worden bedankt voor de vele foto's die zij voor mij hebben afgedrukt. René Koper, Wim Barsingerhorn, Idsart Attema, Henk Veerman, Joop van Wel en vele anderen wilden mij altijd met wat dan ook meteen van dienst zijn.

Experimenteren met Rob Schreutelkamp stond garant voor een zéér snelle en pragmatische aanpak. Zonder hem zou veel van het werk niet hebben plaatsgevonden.

The work with Vito Raineri in Catania, Sicily, introduced me for the first time into a device manufacturing environment. He, and many of his colleagues and friends, also explained me what "Sicilian hospitality" means in practice. I enjoyed my stay there very much.

Het analyseren van device structuren in Twente tesamen met Rutger Wijburg ging soms met veel humor gepaard. Zelden zal men daar zoveel tevredenheid hebben geconstateerd als er weer een transistor 'lek' was.

Als laatste wil ik al mijn kamergenoten bedanken voor het creëren van een prettige en stimulerende werksfeer.



## CURRICULUM VITAE

Op 9 april 1962 ben ik geboren in Leeuwarden. Na het behalen van het HAVO diploma aan de Stedelijke Scholengemeenschap te Leeuwarden begon ik in september 1980 aan de studie Elektrotechniek aan de Hogere Technische School te Leeuwarden. Na een jaar ben ik doorgestroomd naar de studie Elektrotechniek aan de Universiteit Twente. In december 1985 heb ik het kandidaatsexamen afgelegd. Tijdens de doctoraalopleiding heb ik een stage doorlopen in de electriciteitscentrale in Haifa, Israël. Hier moest ik back-up systemen testen en adviseren bij aankoop van nieuwe testapparatuur. Mijn afstudeeropdracht heb ik vervolgens uitgevoerd onder leiding van dr W.C. Sinke en dr L.A. Verhoef op het FOM-instituut voor Atoom- en Molecuulfysica (AMOLF) te Amsterdam. Hier werd een nieuwe methode voor het meten van de levensduur van minderheidsladingsdragers in zonnecellen opgezet en ontwikkeld. In april 1988 behaalde ik het doctoraal examen elektrotechniek bij prof. dr J. Middelhoek.

Vanaf april 1988 voerde ik mijn promotieonderzoek in dienst van de Universteit Twente uit op het AMOLF in de groep Nieuwe Materialen & Zonnecellen van prof. dr F.W. Saris. Onderzocht werden methoden om defectformatie tijdens hoge temperatuur behandelingen van ionen geïmplanteerd silicium tegen te gaan. Een deel van dit werk is beschreven in dit proefschrift.

## PUBLICATIONS

This thesis is based on the following publications:

- Chapter 2: J.R. Liefting, J.S. Custer, R.J. Schreutelkamp, and F.W. Saris, *Dislocation formation in Si implanted at different temperatures*, to be submitted.
- Chapter 3: J.R. Liefting, V.Raineri, R.J. Schreutelkamp, J.S. Custer, *Avoiding dislocation formation for B, P, and As implants in silicon*, Mat. Res. Soc. Symp. Proc. **235**, 173 (1992).
- Chapter 4: J.R. Liefting, J.S. Custer, and F.W. Saris, *C implantation for suppression of dislocation formation*, Mat. Res. Soc. Symp. Proc. **235**, 179 (1992).
- Chapter 5: J.R. Liefting, R.C.M. Wijburg, J.S. Custer, H. Wallinga, and F.W. Saris, *Improved device performance by multi step or Carbon co-implants*, to be submitted.
- Chapter 6: J.R. Liefting, R.J. Schreutelkamp, W.X. Lu and F.W. Saris, *Gettering of Cu at buried damage layers made by silicon self implantation*, Mat. Res. Soc. Symp. Proc. **157**, 641 (1990).

Other publications related to this work:

- L.A. Verhoef, J.R. Liefting, J.C. Stroom, and W.C. Sinke, *New dimensions in minority-carrier lifetime determination on poly-crystalline silicon solar cells*, 8th E.C. Photovoltaic Solar Energy Conf. (Florence, Italy, 9 - 13 May 1988) 102-106.
- W.X. Lu, Y.H. Qian, R.H. Tian, Z.L. Wang, R.J. Schreutelkamp, J.R. Liefting, and F.W. Saris, *Reduction of secondary defect formation in MeV B ion-implanted Si(100)*, Appl. Phys. Lett. **55**, 1838-1840 (1989).
- R.J. Schreutelkamp, J.R. Liefting, P.M. Zagwijn, W.X. Lu, and F.W. Saris, *Range Straggling of MeV Ions in Amorphous Silicon: Discrepancies with TRIM*, Nucl. Instr. and Meth. **B48**, 448-452 (1990).
- R.J. Schreutelkamp, J.R. Liefting, P.M. Zagwijn, W.X. Lu and F.W. Saris, *Addendum to "Range Straggling of MeV Ions in Amorphous Silicon: Discrepancies with TRIM"*, Nucl. Instr. and Meth. **B47**, 329-331 (1990).

- L.A. Verhoef, J.C. Stroom, F.J. Bisschop, J.R. Liefiting, and F.W. Saris, *3D-resolved determination of minority-carrier lifetime in solar cells by photo-current decay*, J. Appl. Phys. **68**, 6485-6494 (1990).
- R.J. Schreutelkamp, W.X. Lu, J.R. Liefiting, V. Raineri, J.S. Custer, and F.W. Saris, *Reduction of secondary defect formation in MeV As-ion implanted Si(100)*, Nucl. Instr. and Meth. Res. **B59/60**, 614-618 (1991).
- R.J. Schreutelkamp, J.S. Custer, J.R. Liefiting and F.W. Saris, *Avoiding pre-amorphization damage in MeV heavy ion-implanted silicon*, Appl. Phys. Lett. **58**, 2827-2829 (1991).
- J.S. Custer, M.O. Thompson, D.J. Eaglesham, D.C. Jacobson, J.M. Poate, J.R. Liefiting, and F.W. Saris, *Epitaxy and nucleation in Cu and Ag doped amorphous Si*, Mat. Res. Soc. Symp. Proc. **205**, 69 (1992).
- R.J. Schreutelkamp, J.S. Custer, J.R. Liefiting, W.X. Lu, and F.W. Saris, *Pre-amorphization damage in ion-implanted silicon*, Mater. Sci. Rept. **6**, 275-366 (1991).
- R.J. Schreutelkamp, J.S. Custer, V. Raineri, J.R. Liefiting, and F.W. Saris, *The role of extended defects on transient B diffusion in ion-implanted silicon*, Mat. Sci. and Eng. **B12**, 307 (1992).
- R.J. Schreutelkamp, J.S. Custer, J.R. Liefiting, F.W. Saris, W.X. Lu, B.X. Zhang, and Z.L. Wang, *Pre-amorphization damage in Si(100) implanted with high mass MeV ions*, proceedings EMRS 1991, in press.
- J.R. Liefiting, J.S. Custer, R.J. Schreutelkamp, and F.W. Saris, *Dislocation formation in Si implanted at elevated temperature*, in: Proceedings International School of Materials Science and Technology, Erice, 1991, in press.
- J. Klappe, I. Barsony, J.R. Liefiting, and T.W. Ryan, *Optimization of annealing of implant damage by means of High-Resolution X-ray Diffraction*, to be submitted.

